Physics Highlight: Measurements of $\gamma_v p \rightarrow \pi^+\pi^- p'$ Cross Sections with the CLAS Detector for Q^2 from 2.0-5.0 GeV^2 and W from 1.4-2.1 GeV

Ralf W. Gothe

UNIVERSITY OF SOUTH CAROLINA

Fall CLAS Collaboration

November 17-20, 2026, Newport News, VA

clas

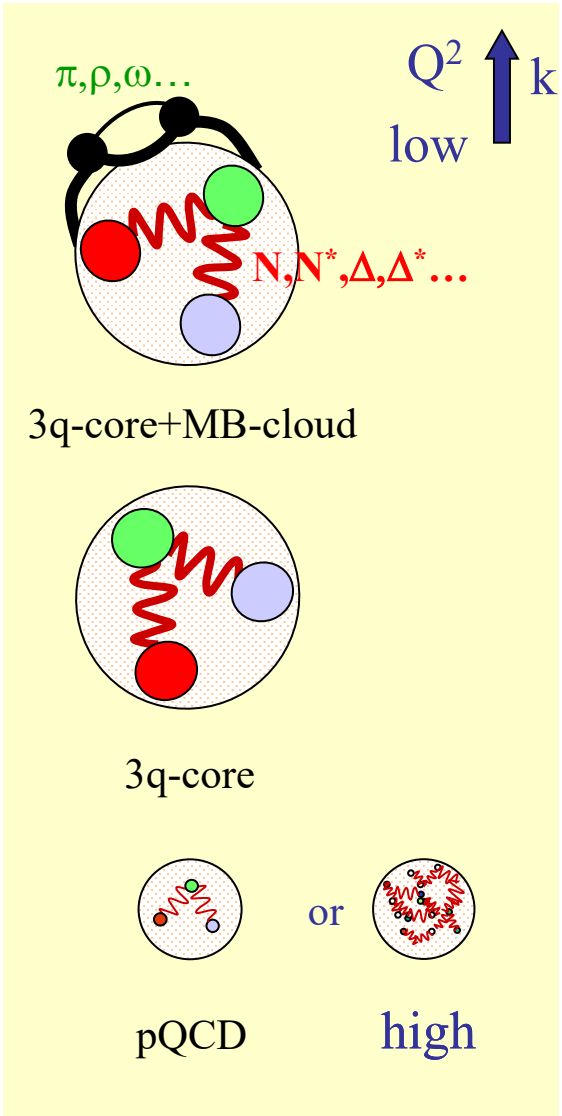
CEBAF Large Acceptance Spectrometer

- Why are γ_vNN* Electrocouplings Interesting? Probe bound valence quarks, potentially diquarks, the emergence of mass, and finally strong QCD.
- Experimental Foundation: Measure cross sections to reveal the space-time-dependent bound quark structure of baryons in various quantum configurations (I, J^π).
- Phenomenological Analyses / Theoretical Impact: Consistent extraction of γ_vNN* electrocouplings / mapping QCD continuously from sQCD towards pQCD.

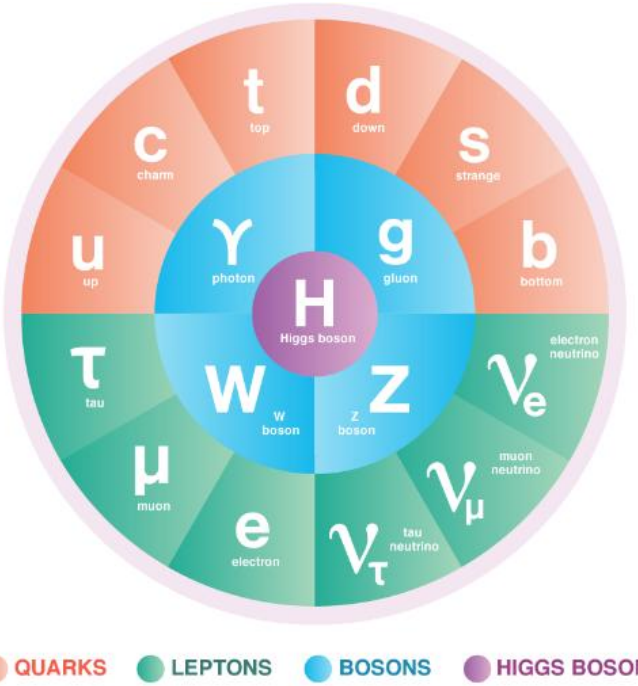
This work is supported in parts by the National Science Foundation under Grant PHY 10014377.

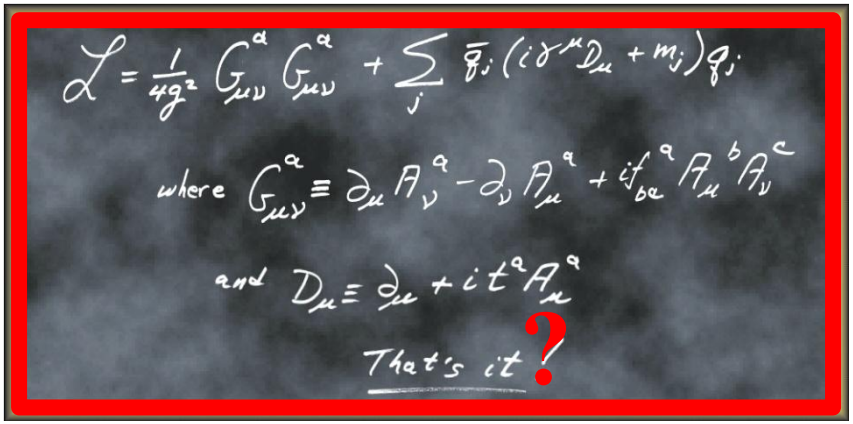
Why is it Interesting?

Emergence of Hadron Mass Traced by Electromagnetic Probes



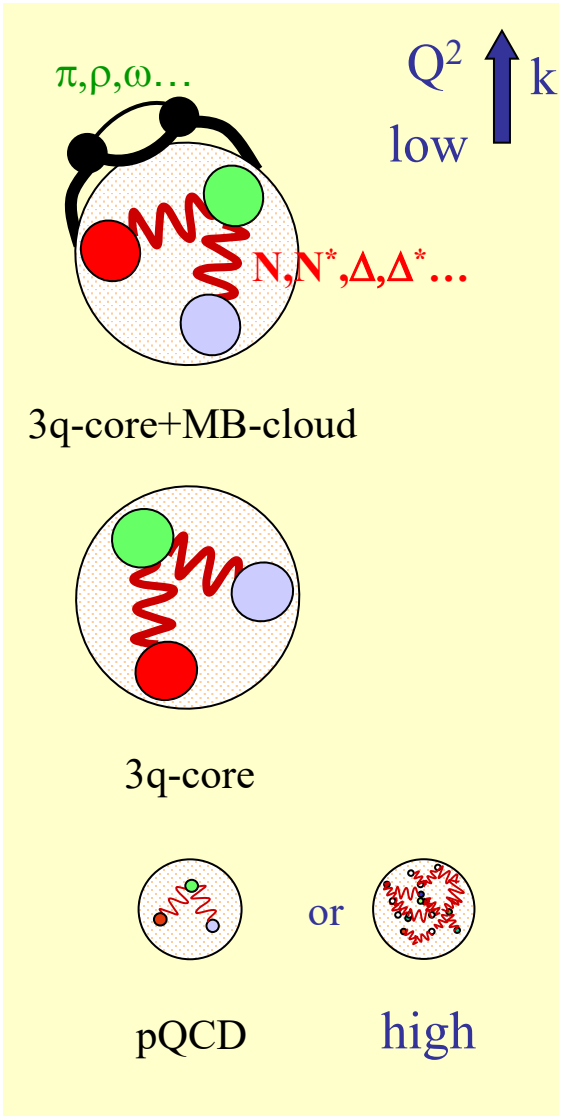
SM



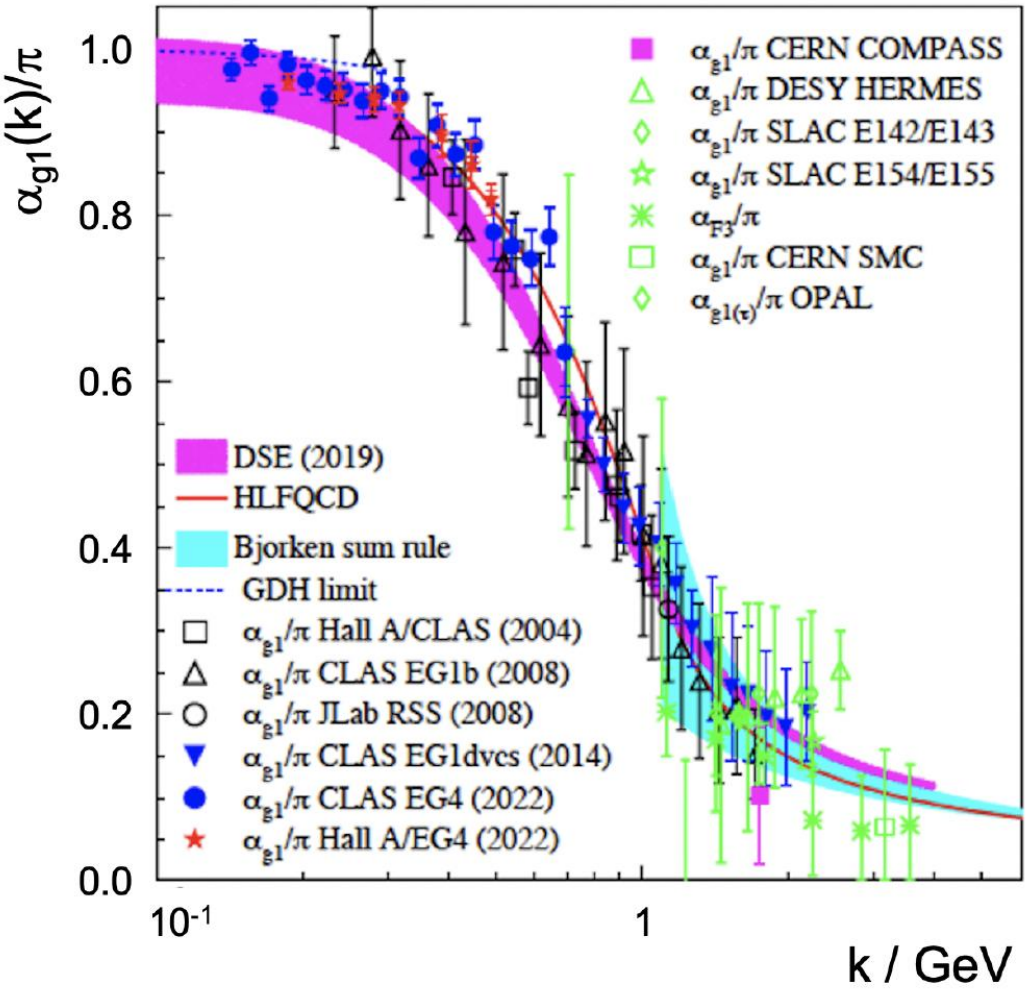


Frank Wilczek, Physics Today, August 2000

Hadron Structure with Electromagnetic Probes



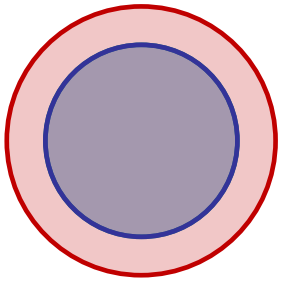
- The SM α_s diverges as Q^2 approaches zero, but confinement and the meson cloud heal this artificial divergence as QCD becomes non-perturbative.



Probing pQCD Experimentally

How can one probe pQCD experimentally when measuring hadrons in the final state?

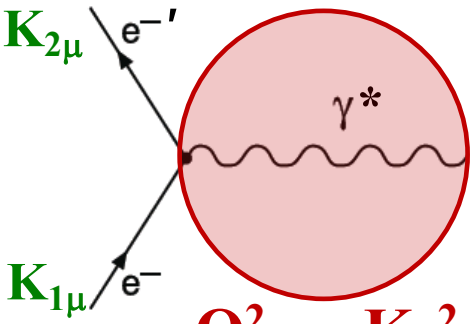
$\langle \psi_f | \mathcal{H}_{\rm int} | \psi_i \rangle$



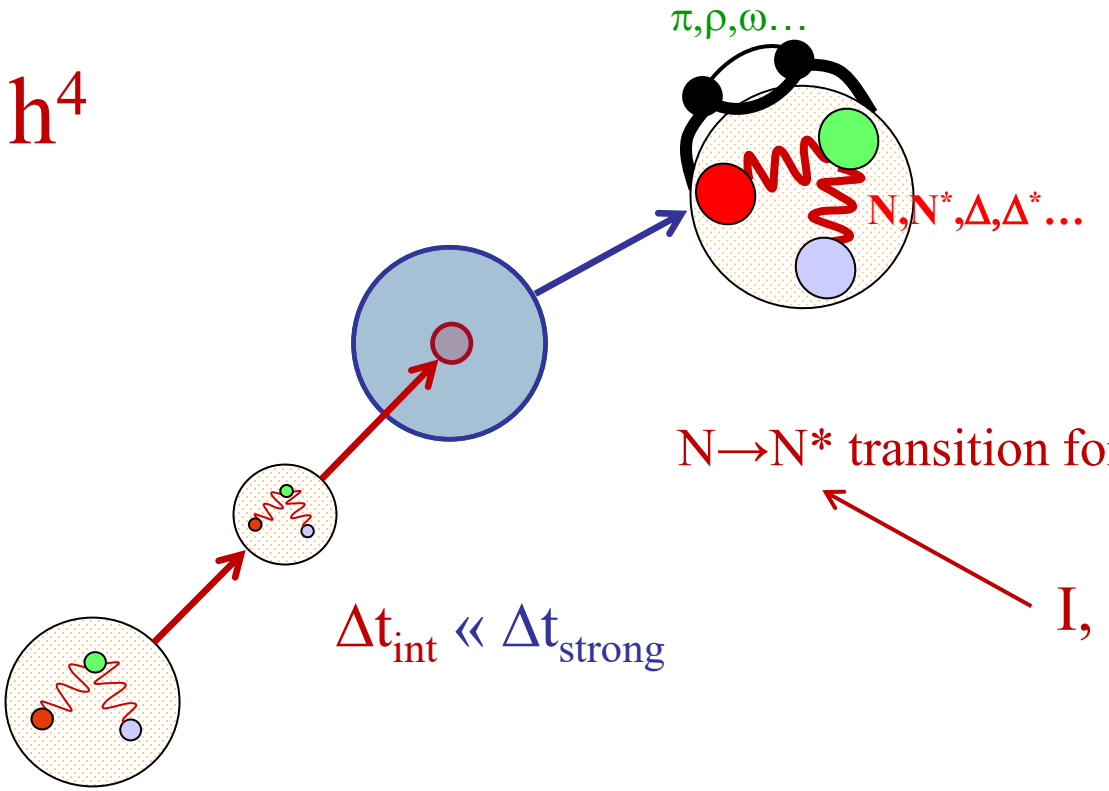
h^3 $\Delta E \to 0$ and $\Delta t \to \infty$

Elastic nuclear form factors

h^4



$Q^2 = -K_\mu^2$

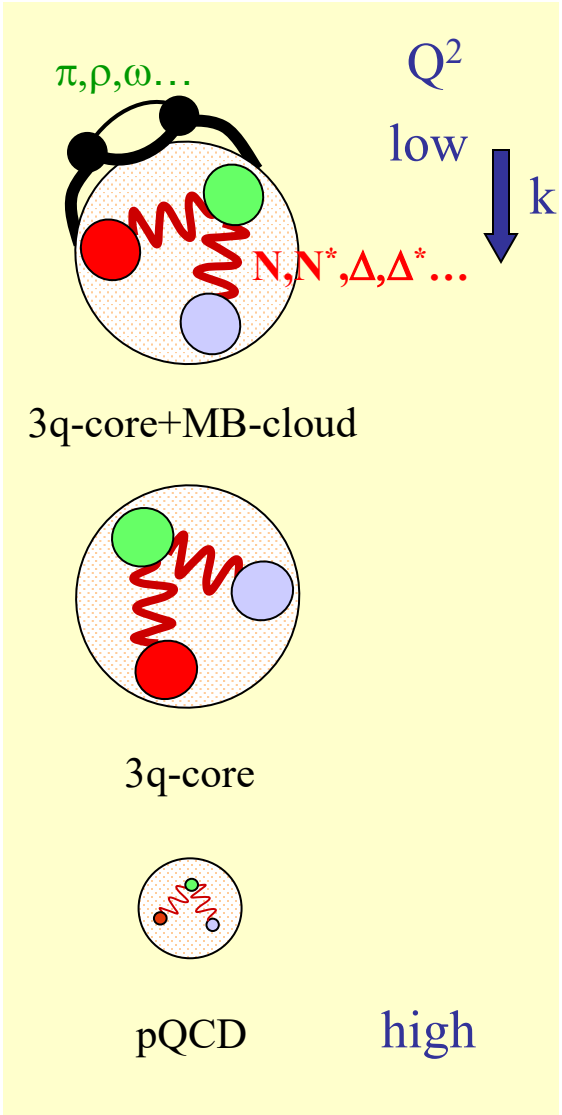


$\Delta t_{\rm int} \ll \Delta t_{\rm strong}$

N→N* transition form factors

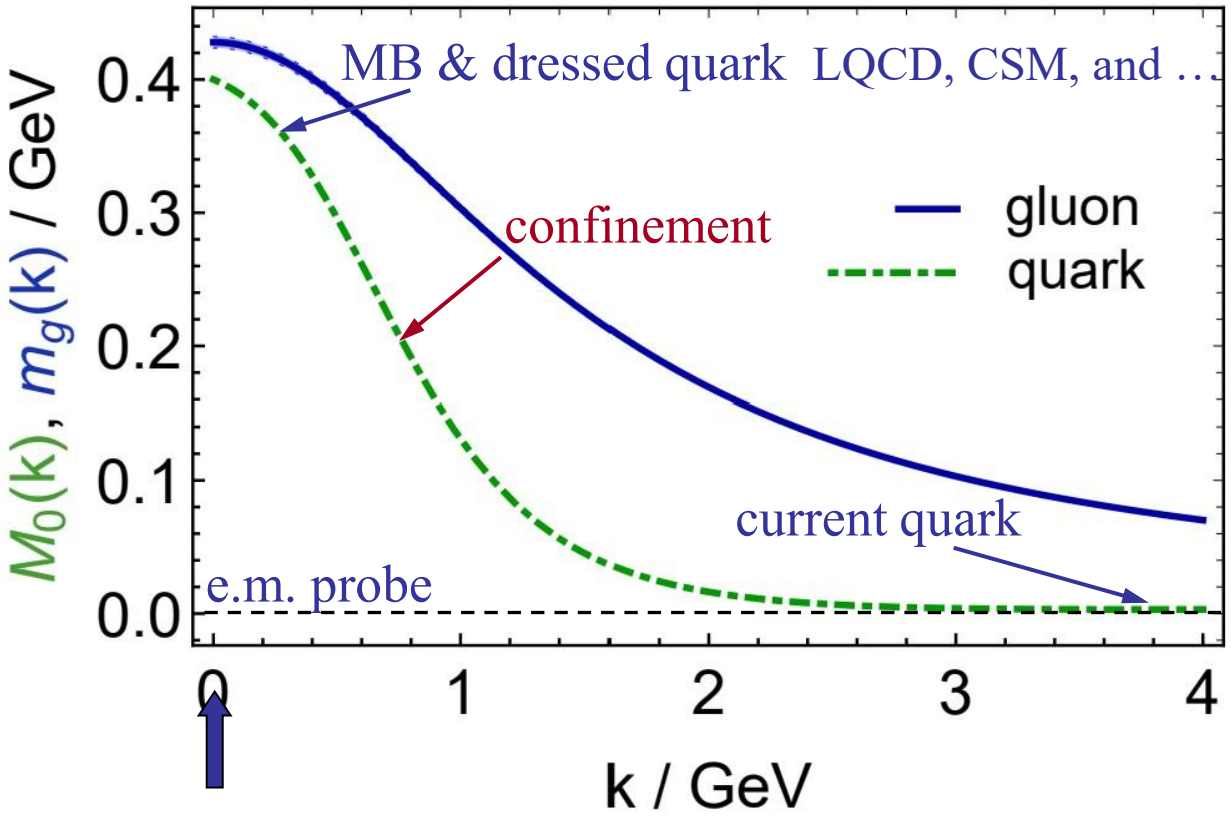
I, J^π

Emergence of Hadron Mass Traced by Electromagnetic Probes

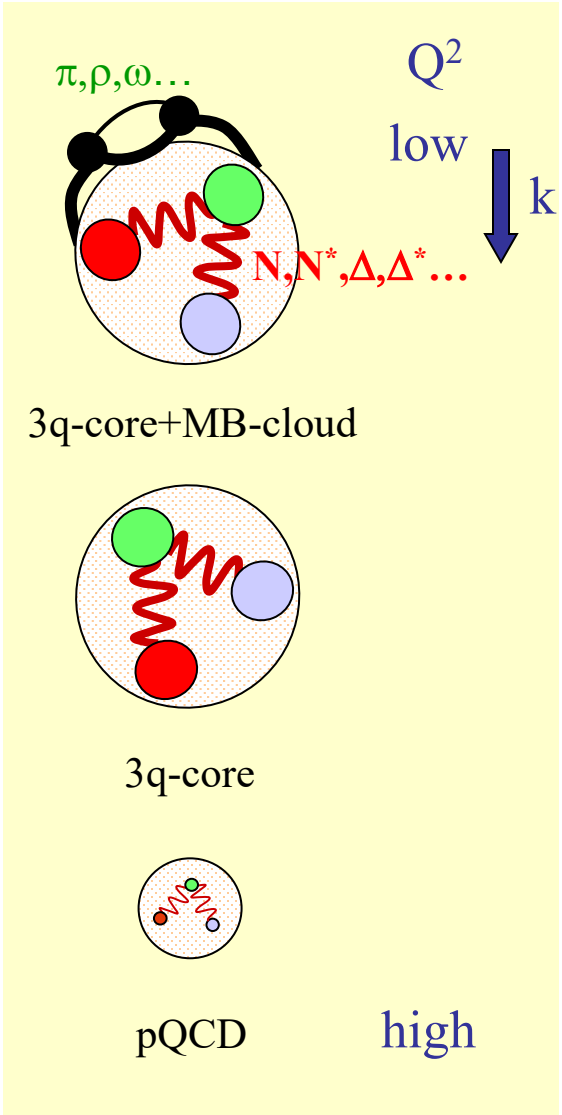


- Study the structure of the nucleon spectrum in the domain where most of the mass is generated by the strong field and dressed quarks are the major active degree of freedom.

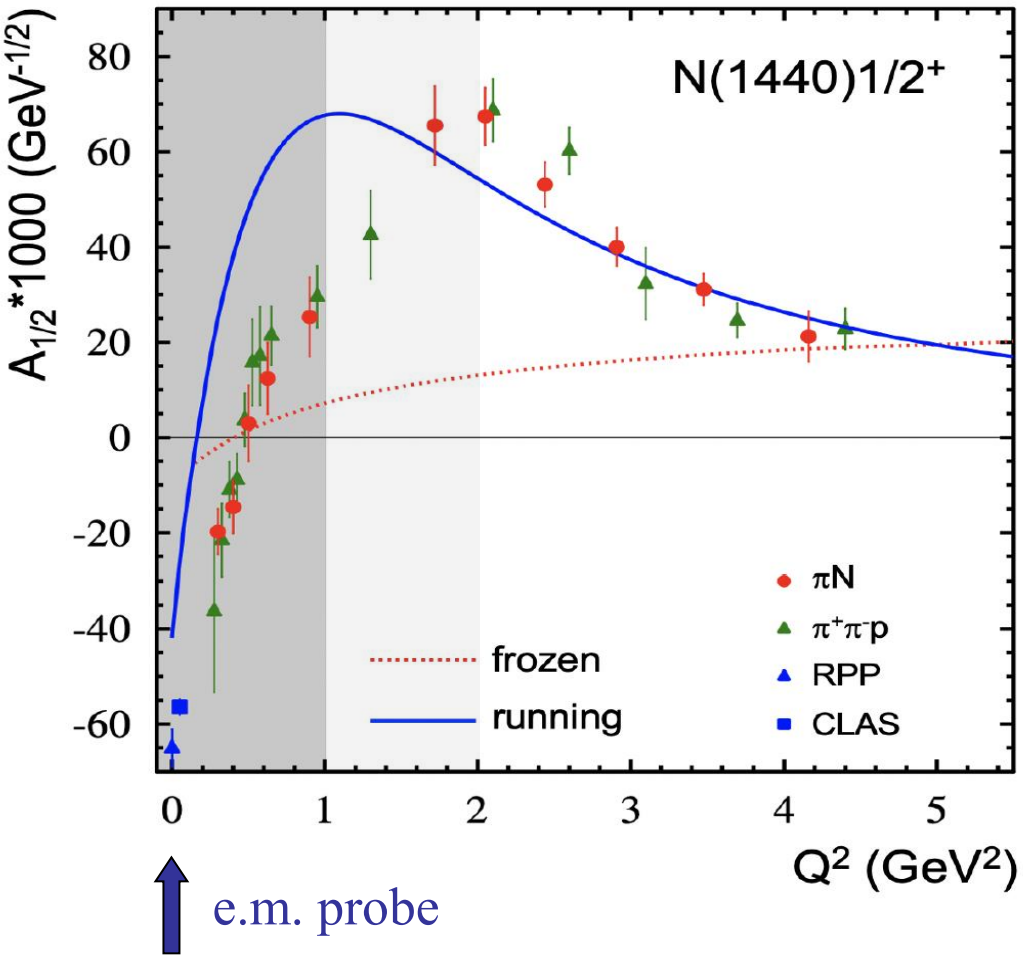
Zhu-Fang Cui et al., Chin. Phys. C **44** (2020) 083102/1-10



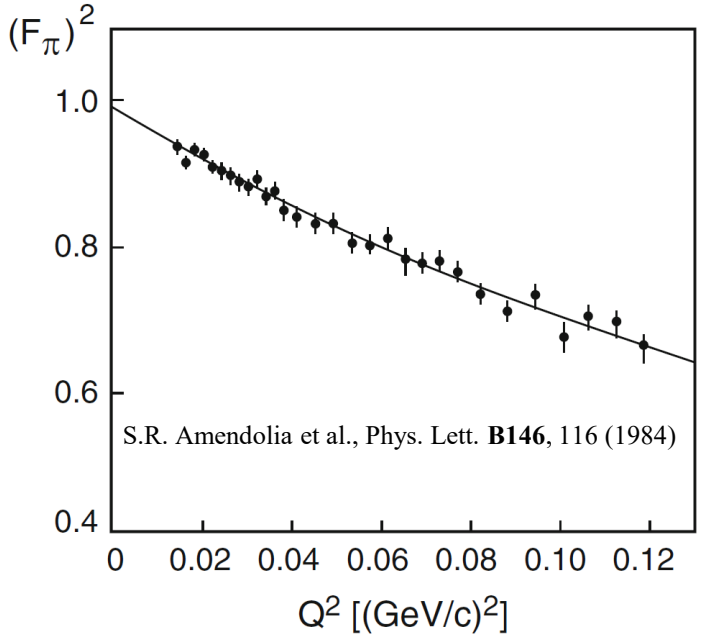
Emergence of Hadron Mass Traced by Electromagnetic Probes

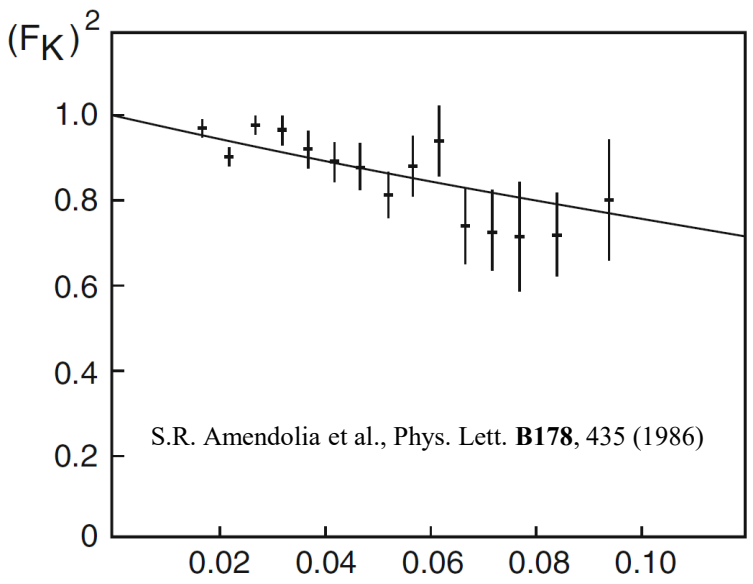


- Study the structure of the nucleon spectrum in the domain where dressed quarks are the major active degree of freedom.

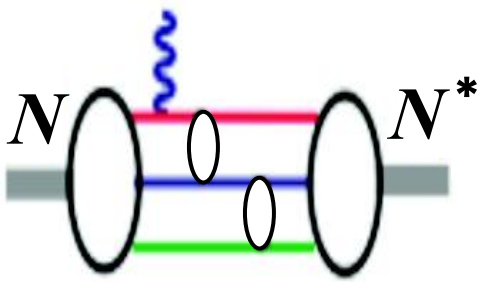


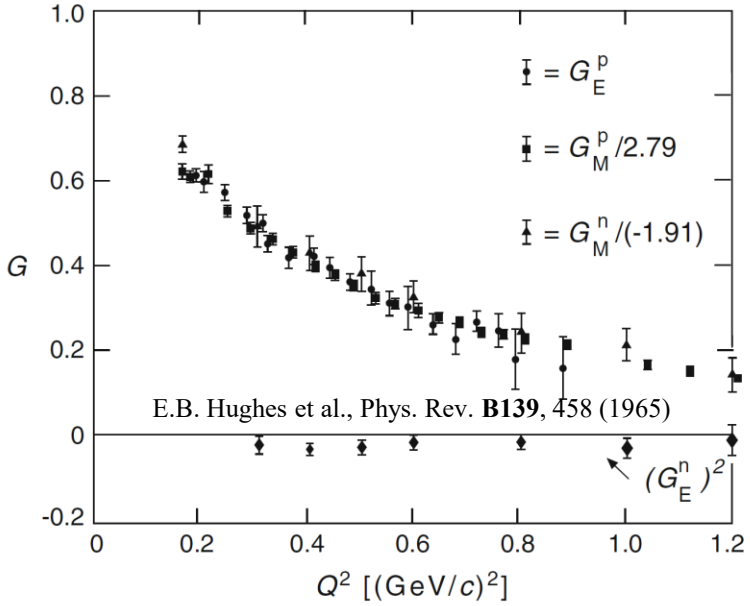
History of Form Factors



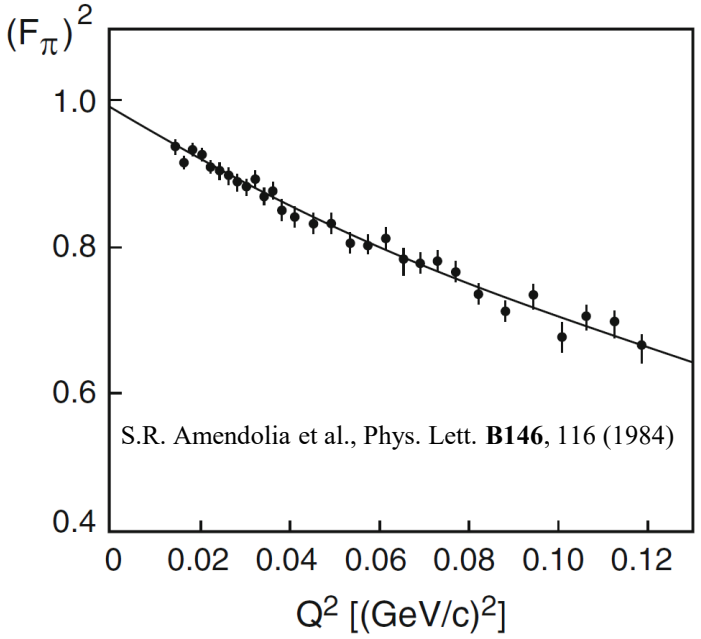


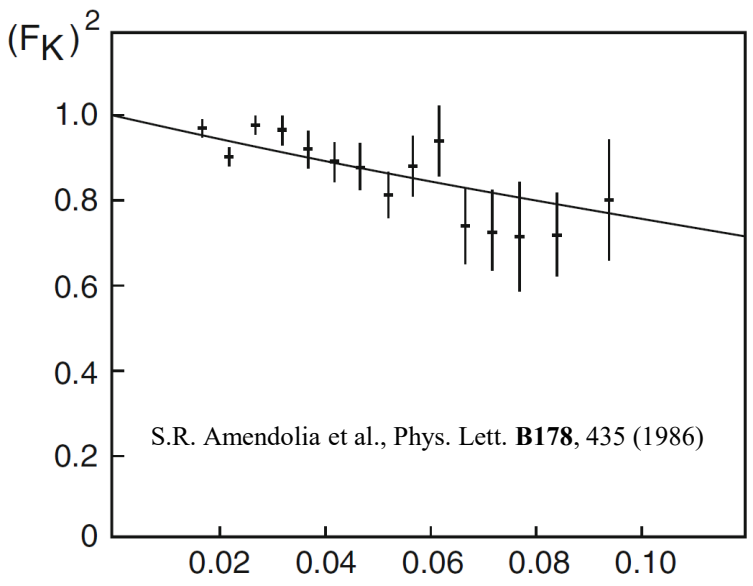
$$F(Q^2) = G_E(Q^2) = \left(1 + Q^2/a^2\hbar^2\right)^{-2}$$





History of Form Factors

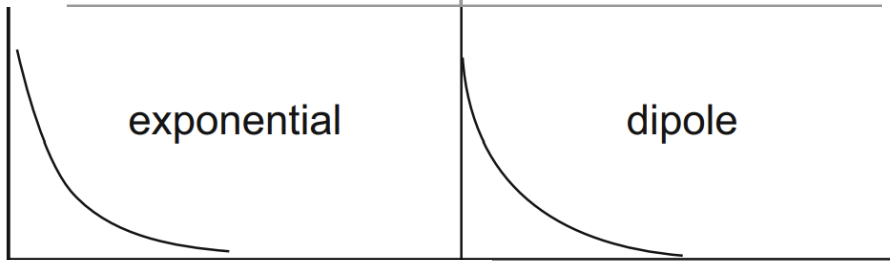


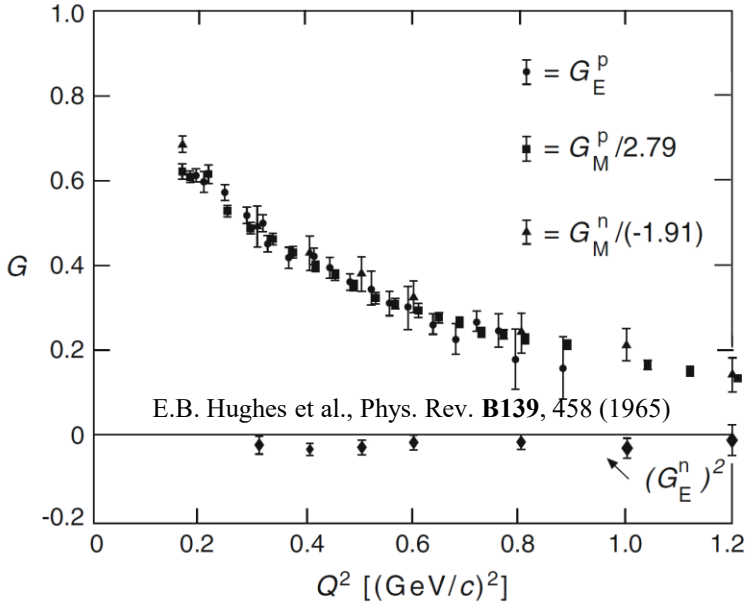


$$F(Q^2) = G_E(Q^2) = \left(1 + Q^2/a^2\hbar^2\right)^{-2}$$

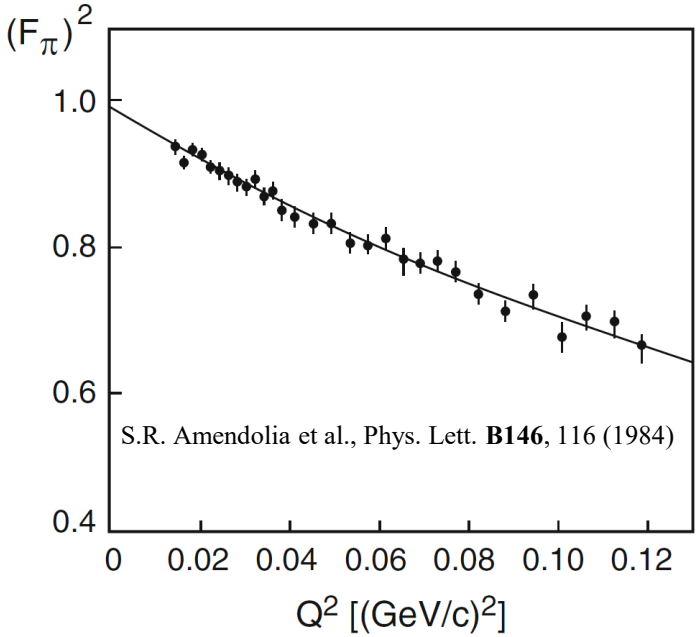
MB or qqq

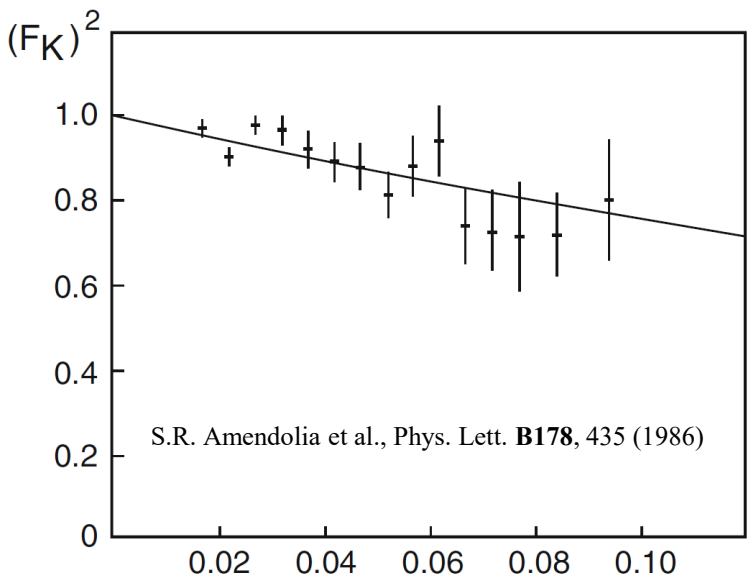
Exponential	$(a^3/8\pi)\cdot\exp(-ar)$



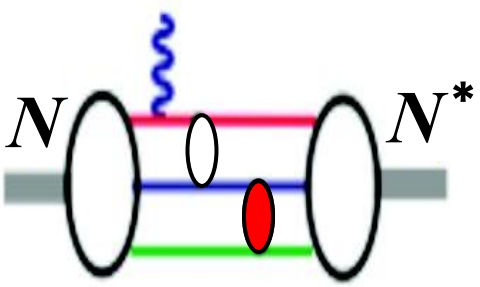


History of Form Factors

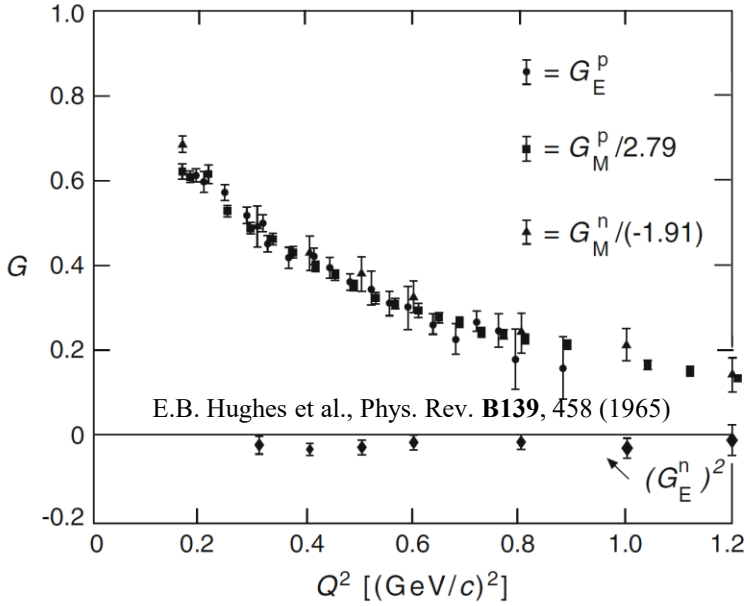




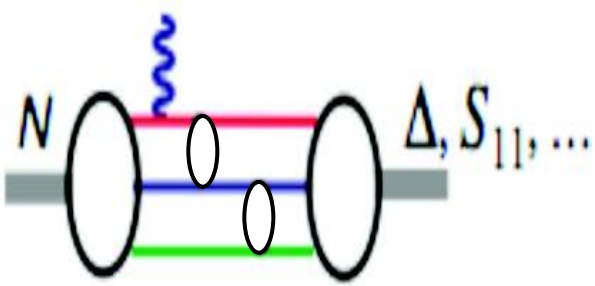
$$F(Q^2) = G_E(Q^2) = \left(1 + Q^2/a^2\hbar^2\right)^{-2}$$



$$F(Q^2) = \left(1 + Q^2/a^2\hbar^2\right)^{-1} * \left(1 + Q^2/a_d^2\hbar^2\right)^{-1}$$

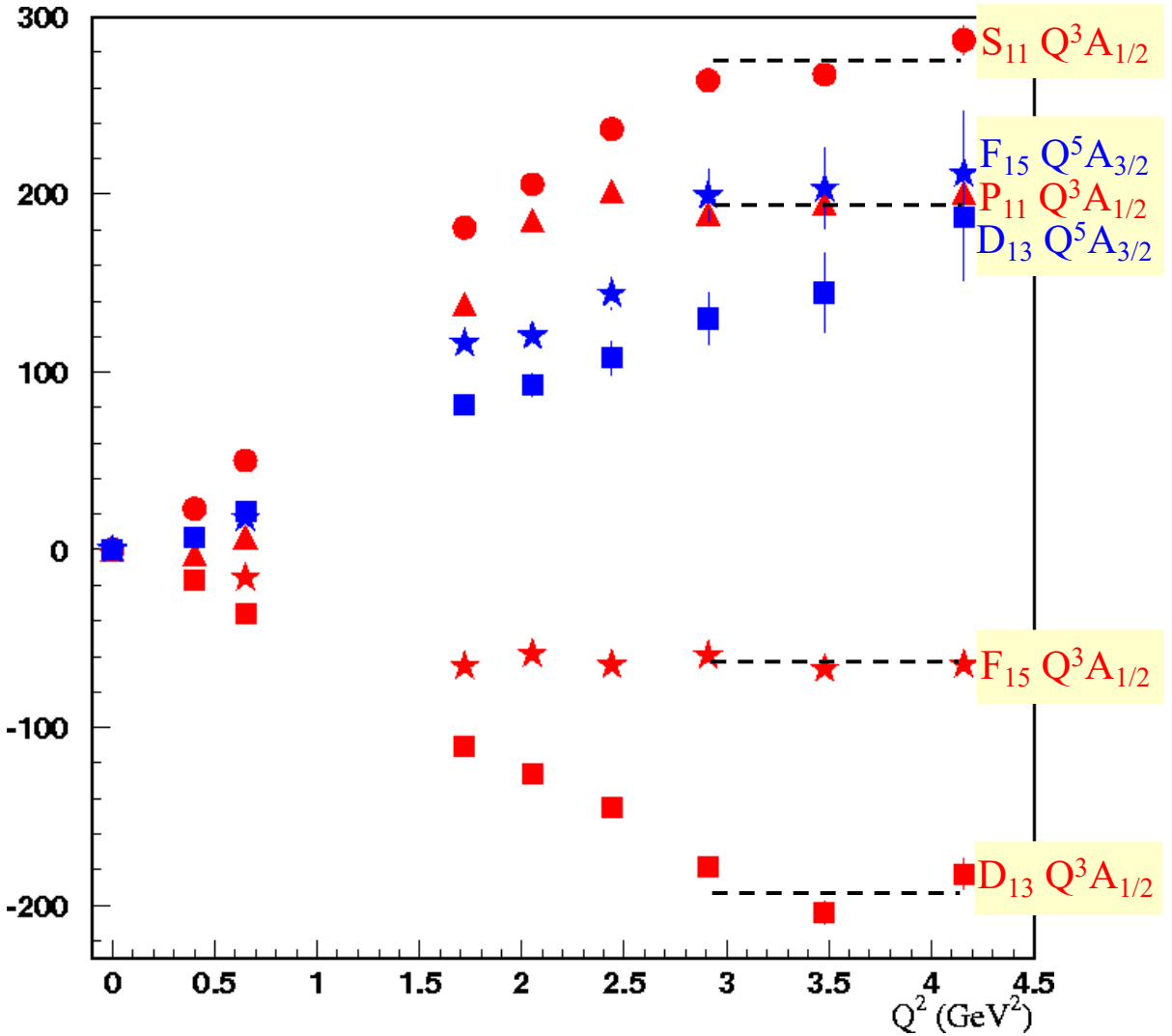


Evidence for the Onset of Precocious Scaling?



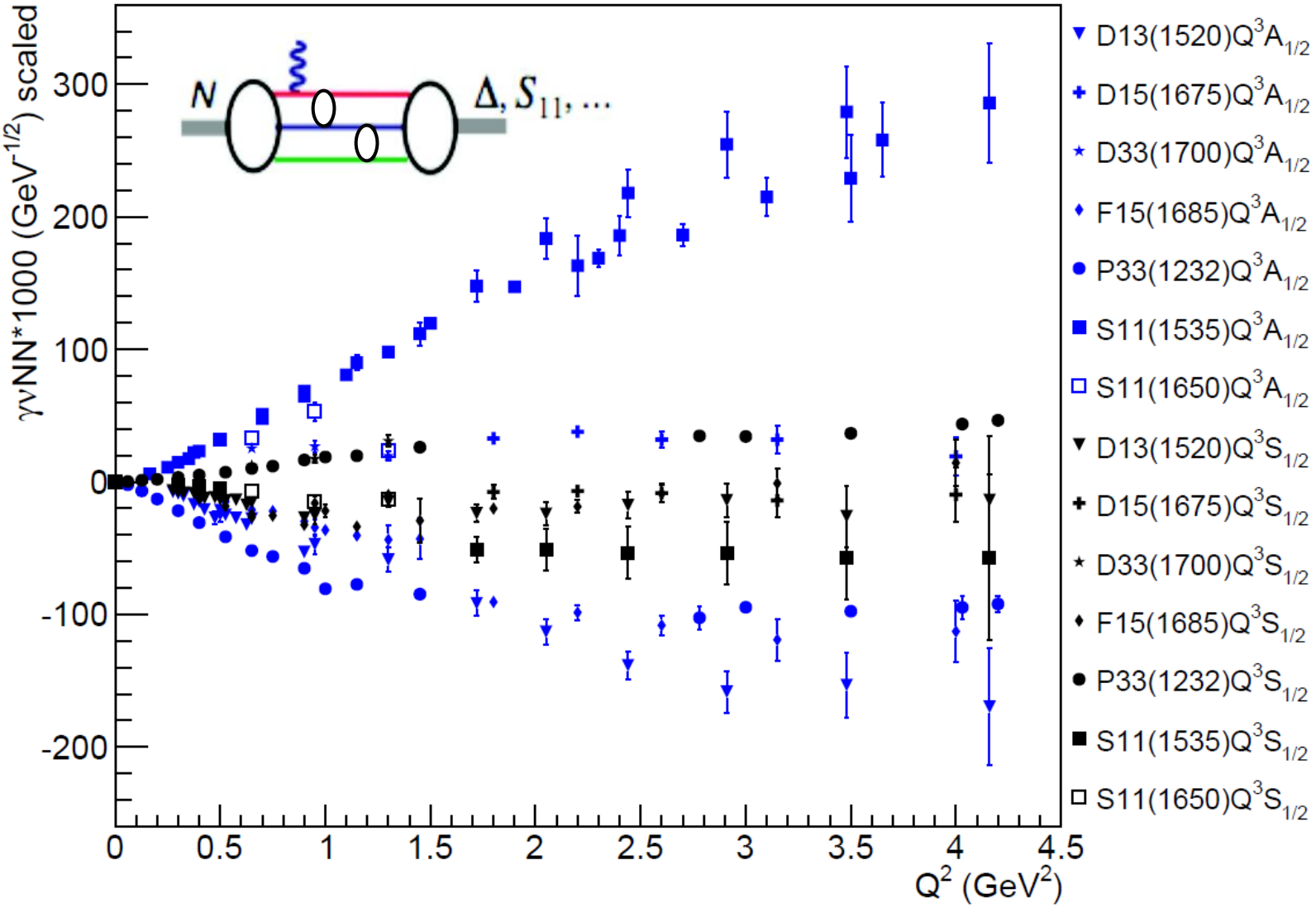
- $A_{1/2} \alpha 1/Q^3$
- $A_{3/2} \alpha 1/Q^5$

I. G. Aznauryan *et al.*, Phys. Rev. C80, 055203 (2009)



Evidence for the Onset of Precocious Scaling?

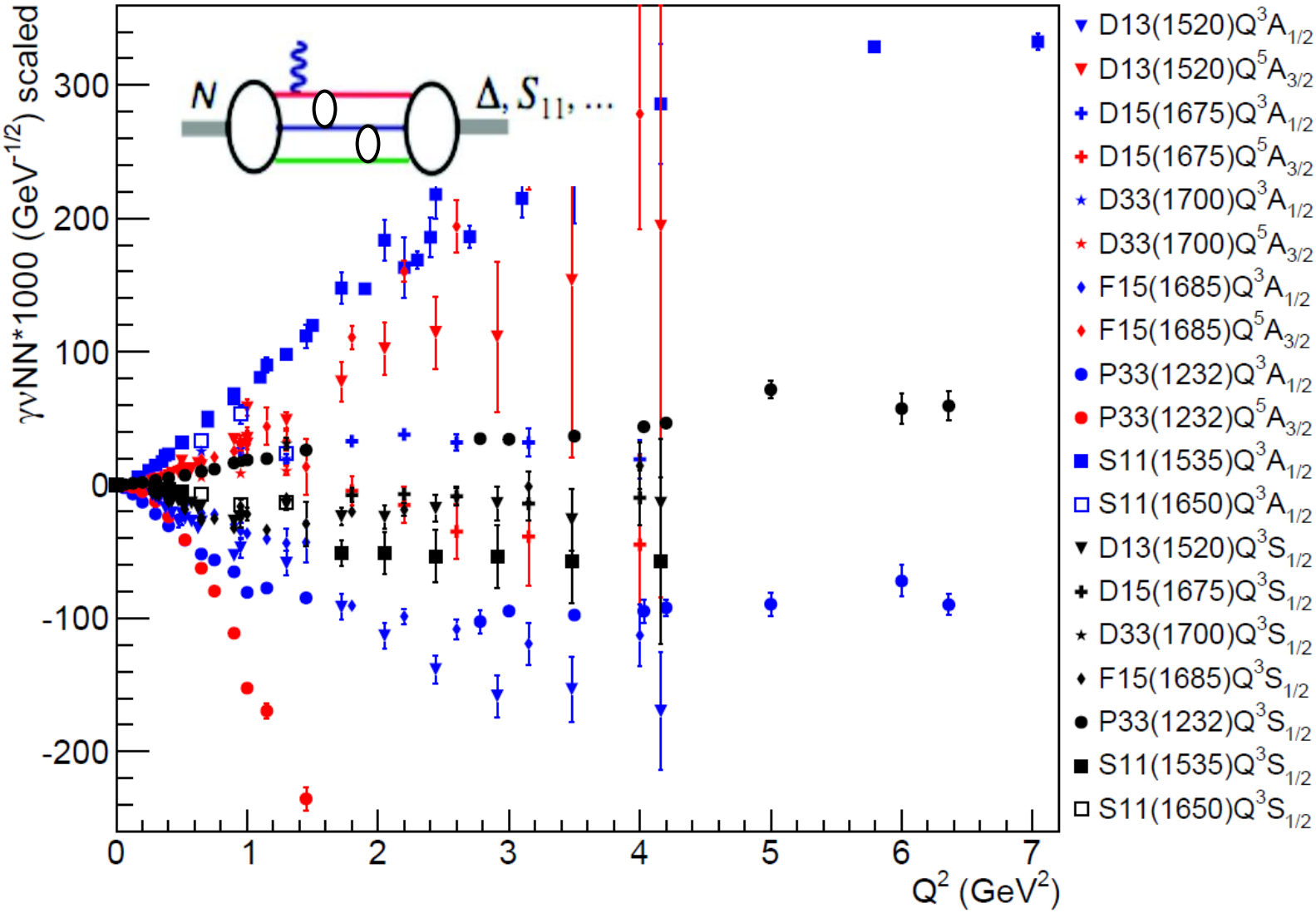
Ye Tian



V. Mokeev, userweb.jlab.org/~mokeev/resonance_electrocouplings/ (2016)

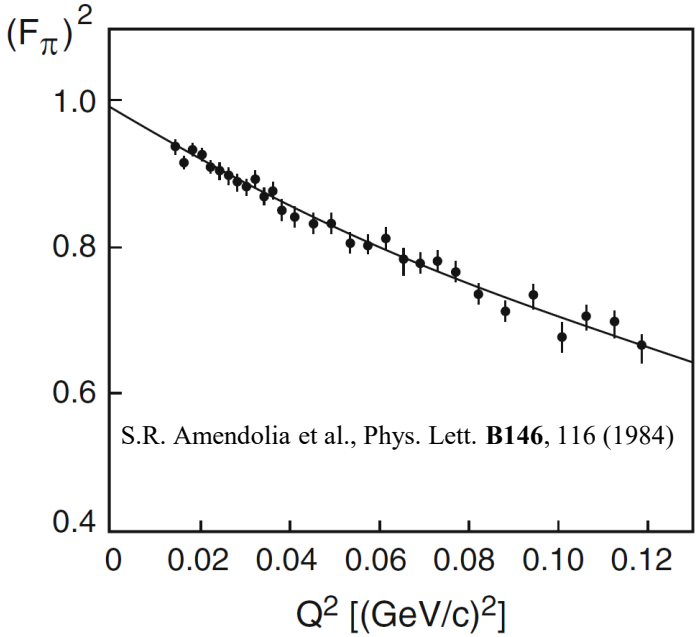
Evidence for the Onset of Precocious Scaling?

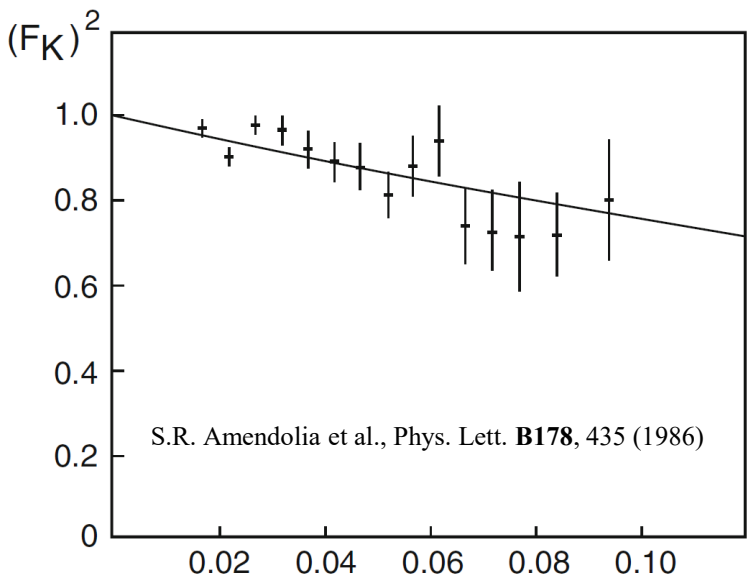
Ye Tian



V. Mokeev, userweb.jlab.org/~mokeev/resonance_electrocouplings/ (2016)

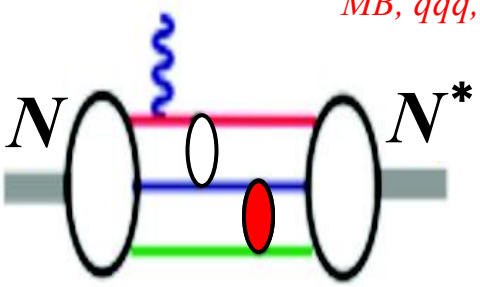
History of Form Factors



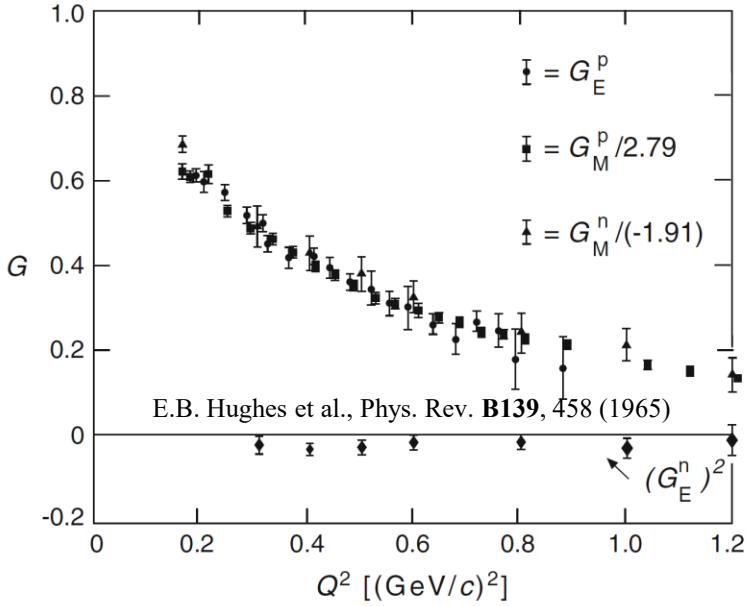


$$F(Q^2) = G_E(Q^2) = \left(1 + Q^2/a^2\hbar^2\right)^{-2}$$

MB, qqq, or qd

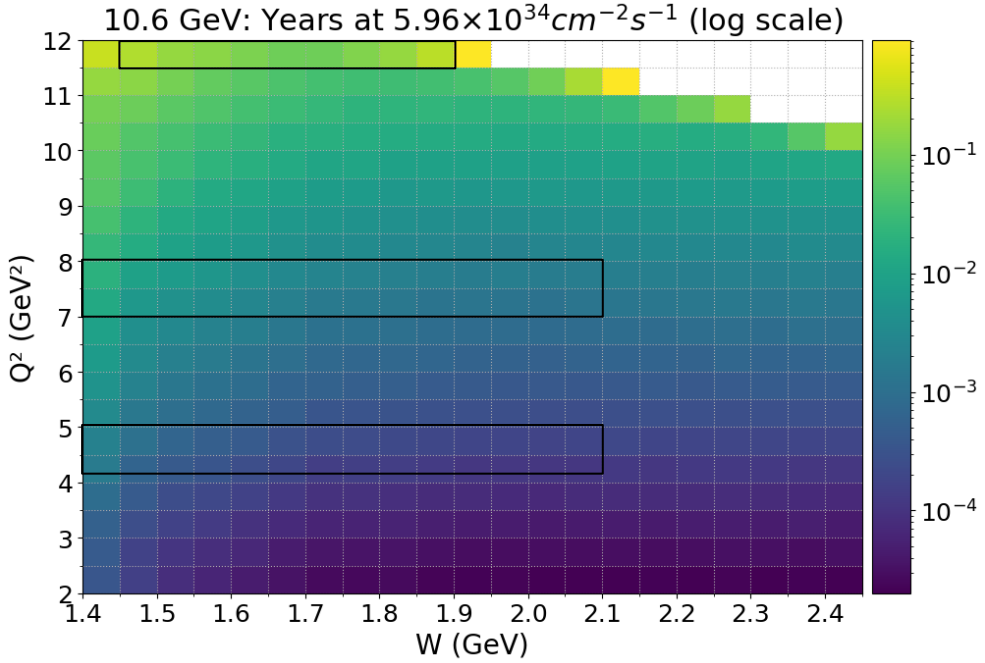


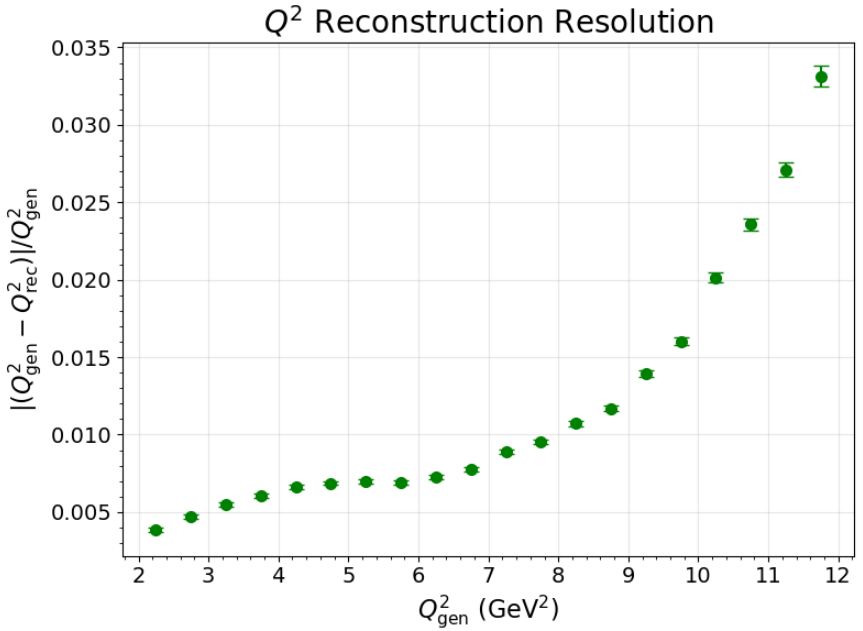
$$F(Q^2) = \left(1 + Q^2/a^2\hbar^2\right)^{-1} * \left(1 + Q^2/a_d^2\hbar^2\right)^{-1}$$



High Luminosity Opportunities

Alexis Osmond





At 10.6 GeV: Implementing all analysis cuts [3/2], Golden Run Selection [3], PAC Days [2].

Current luminosity (5.96×10^{34} cm^{-2} s^{-1}):	1 year	
Conservatively upgraded luminosity (2×10^{35} cm^{-2} s^{-1}):	4 months	increased # of Q^2 bins
Stage 1 upgraded luminosity (5×10^{35} cm^{-2} s^{-1}):	4 months	3–15 × higher statistics
Stage 2 upgraded luminosity (1×10^{36} cm^{-2} s^{-1}):	4 months	6–30 × higher statistics

Victor Mokeev (Thursday)

High Luminosity Opportunities

Raffaella De Vita

Upgrade path: Stage I

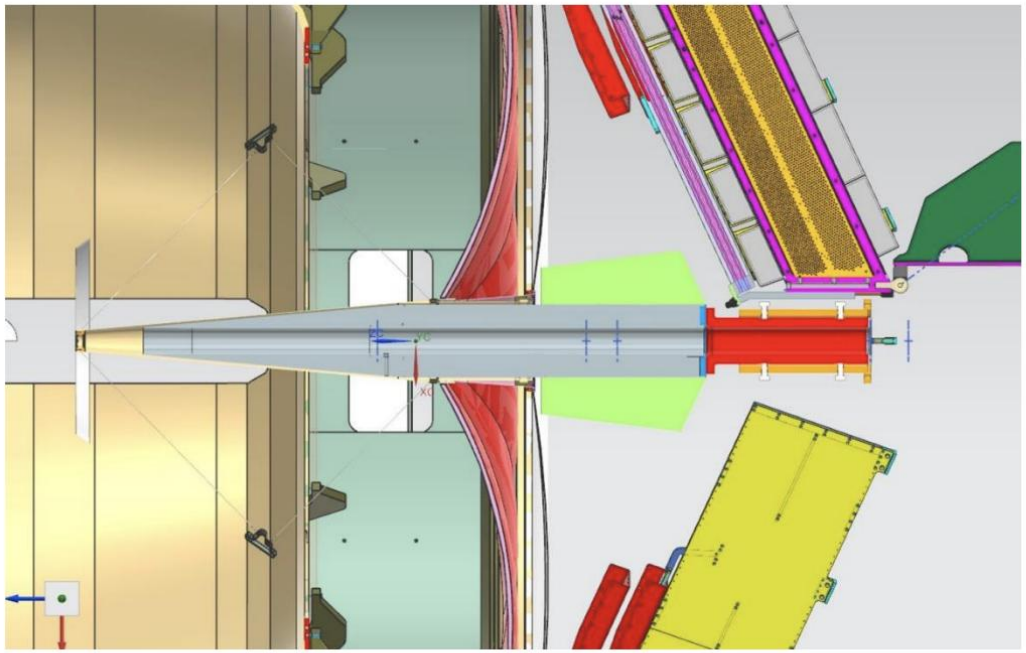
Stage I
7° Møller cone, no Forward Tagger
up to 5 x10^{35} cm^{-2}s^{-1}

➡

Stage II
wECal + Pb shield, 7°–15°,no HTCC
up to 10^{36} cm^{-2}s^{-1}

➡

Stage III = μCLAS12
full FD shield and wCal
10^{37} cm^{-2}s^{-1}



Stage I layout: large Møller cone up to 7°

Configuration

- Large Møller cone, as used for RG-C, with extension to 7°
- Forward Tagger removed
- Luminosity up to 5 x10^{35} cm^{-2}s^{-1} (×5 design)

Required upgrades

- Replace the MicroMegas of the CVT
- New forward vertex tracker (FVT)
- Better shielding downstream of the torus for DC Region 3

Physics

- Most exclusive and semi-inclusive reactions at high Q^2

High Luminosity Opportunities

Raffaella De Vita

Upgrade path: Stage II

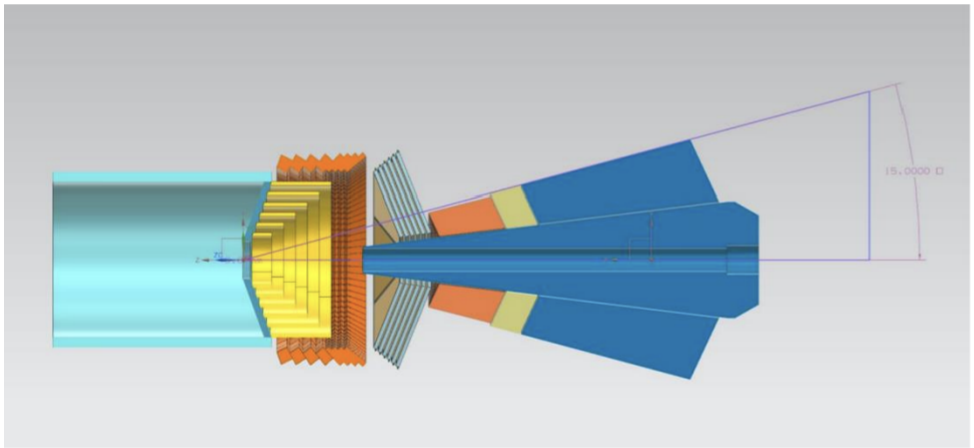
Stage I
7° Møller cone, no Forward Tagger
up to 5 x10^{35} cm^{-2}s^{-1}

→

Stage II
wECal + Pb shield, 7°–15°,no HTCC
up to 10^{36} cm^{-2}s^{-1}

→

Stage III = μCLAS12
full FD shield and wCal
10^{37} cm^{-2}s^{-1}



Stage II layout: wECal and Pb shield from 7° to 15°

Simulation studies

- Luminosity up to 10^{36} cm^{-2}s^{-1}, based on estimated background levels
- First estimates for J/ψ production on neutron

Configuration

- wECal + Pb shield from the 7° Møller cone to 15°
- HTCC removed

Physics

- CLAS12 program, limited to high-rate kinematics
- J/ψ quasi-real photoproduction tagging the recoil nucleon
- Deuteron target: separate bound neutron and proton
- Possible first DDVCS measurements

Operations

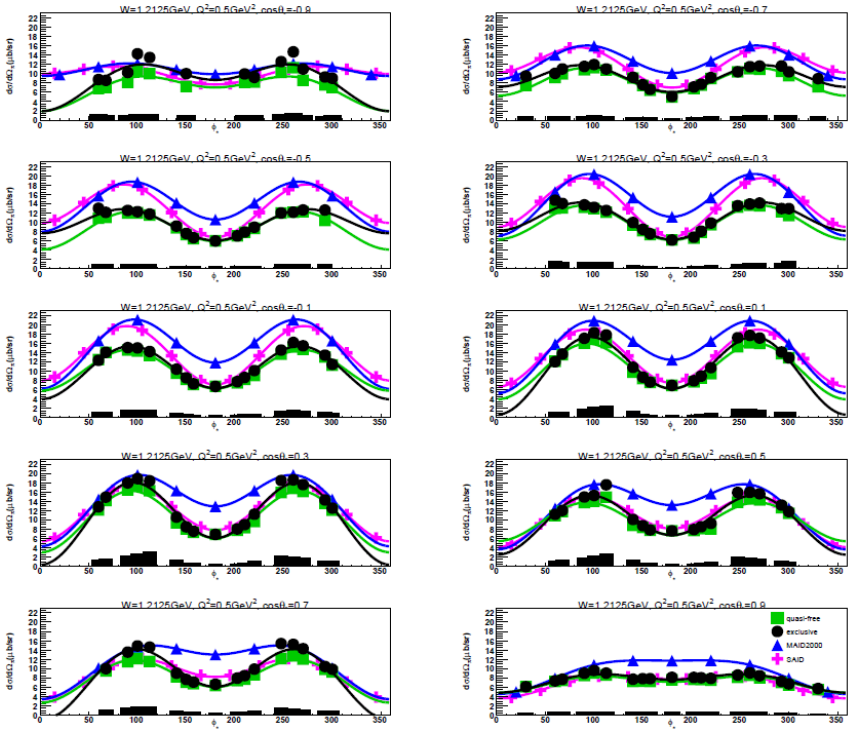
- Experience running with μA beam currents

Experimental Foundation

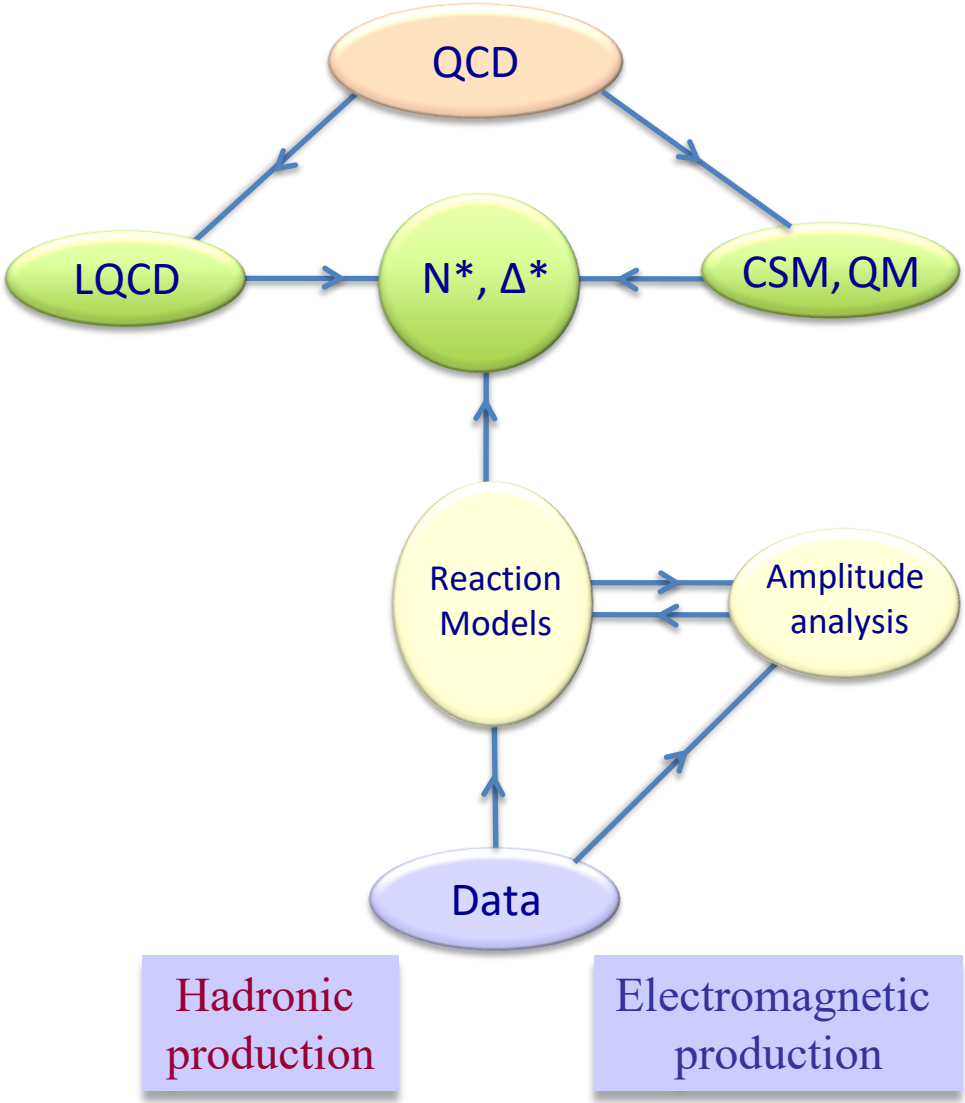
Data-Driven Data Analyses

Consistent Results

Single Pion



Y. Tian *et al.*, Phys. Rev. C 107, 015201 (2023) 26



Exclusive Single π^- Electroproduction off the Deuteron

Ye Tian

W = 1.2125 GeV

ΔW = 25 MeV

Q^2 = 0.5 GeV^2

ΔQ^2 = 0.2 GeV^2

cos(θ) = -0.7

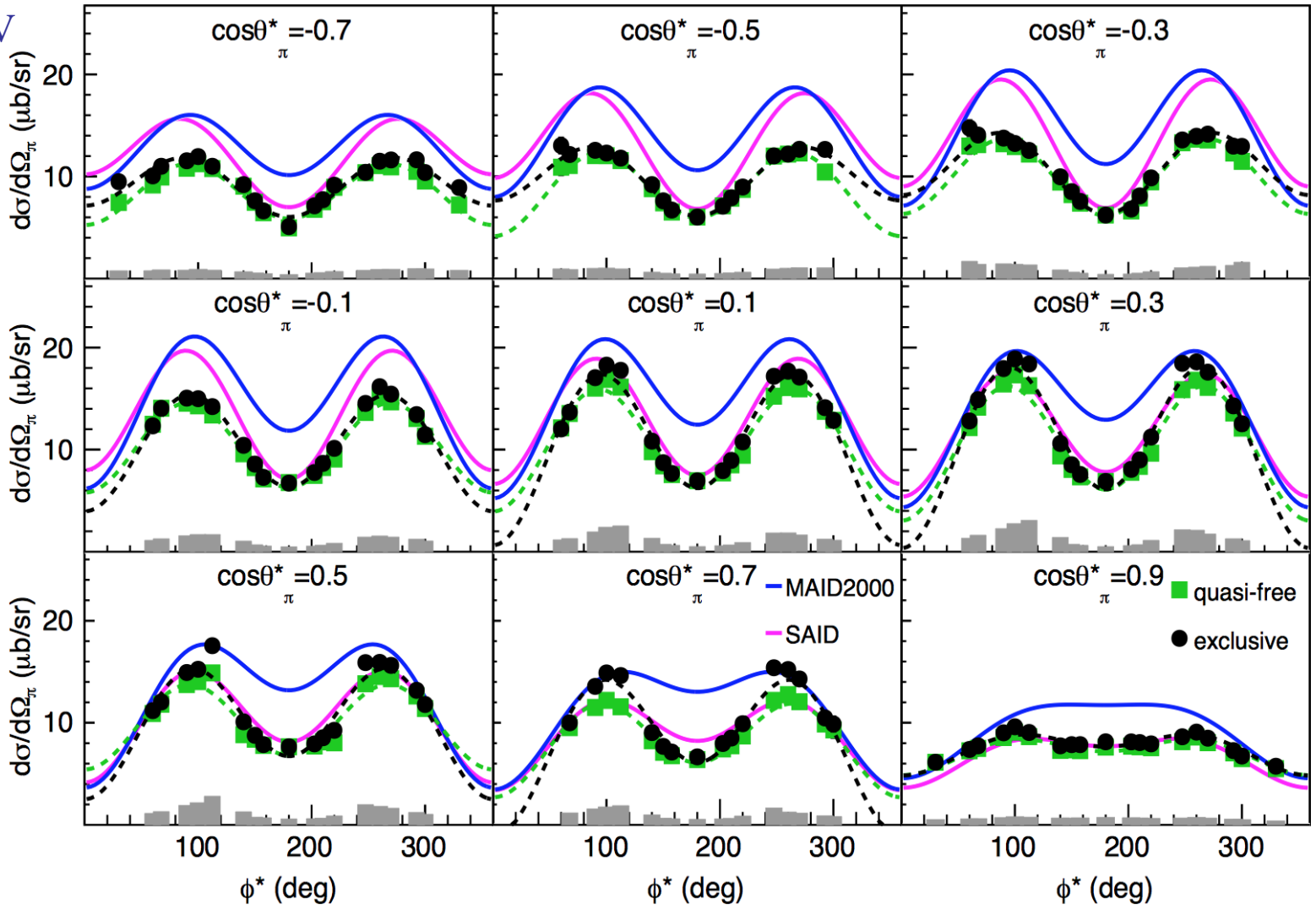
Δcos(θ) = 0.2

cos(θ) = 0.9

ϕ = 20°

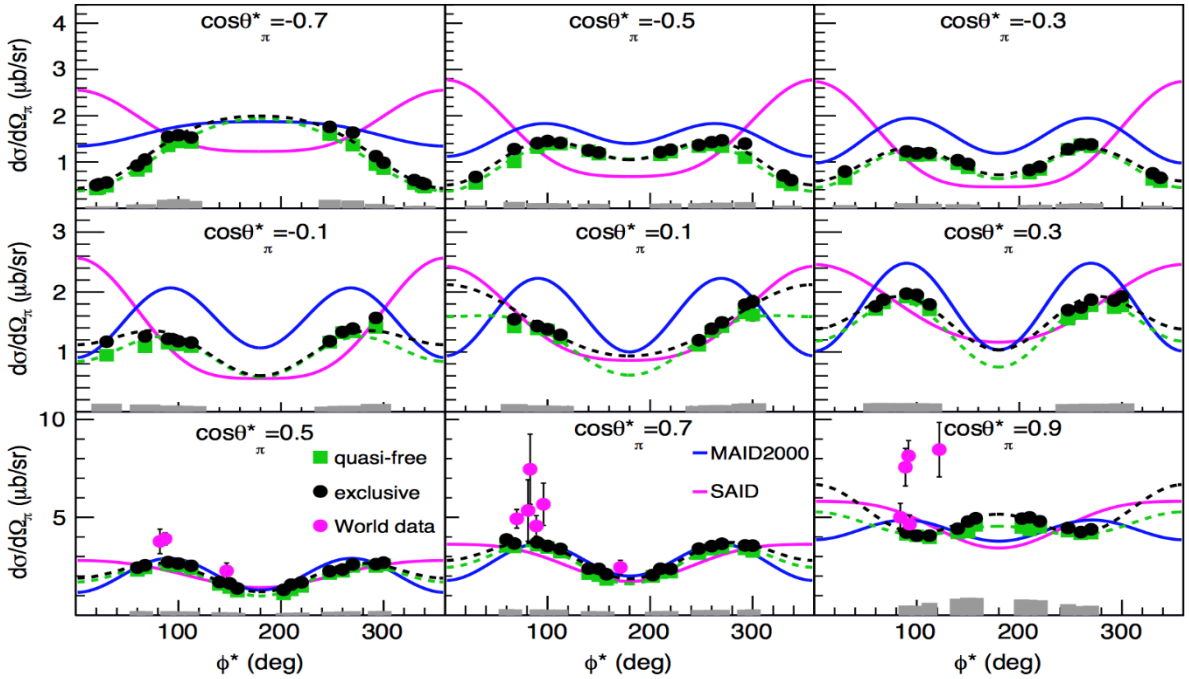
Δϕ = 40°

ϕ = 340°



Exclusive Single π^- Electroproduction off the Deuteron

Ye Tian

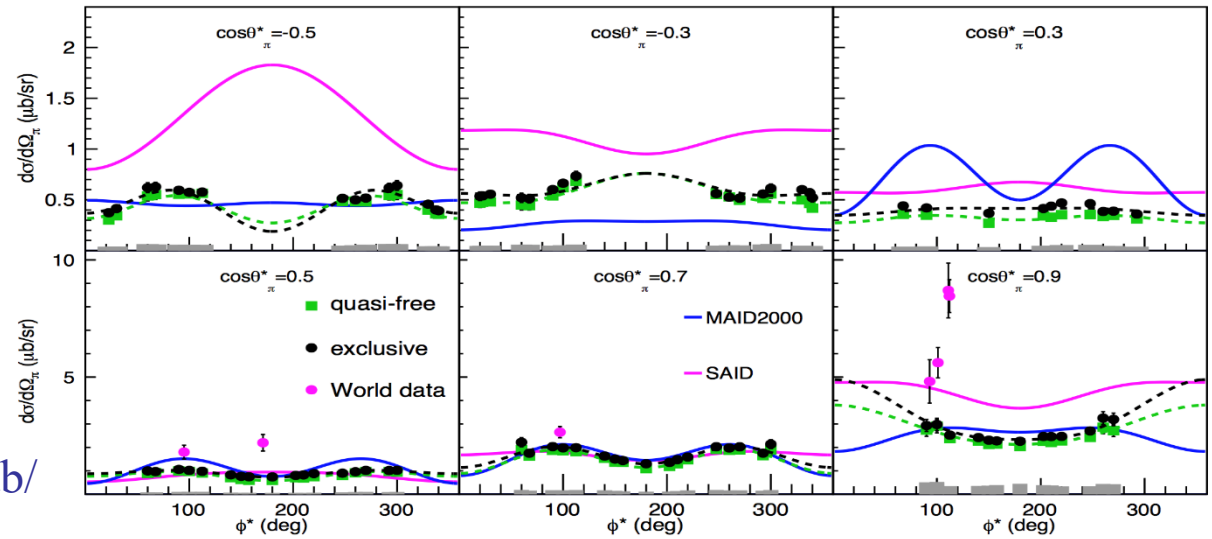


W = 1.5125 GeV

$Q^2 = 0.5\ GeV^2$

$\Delta Q^2 = 0.2\ GeV^2$

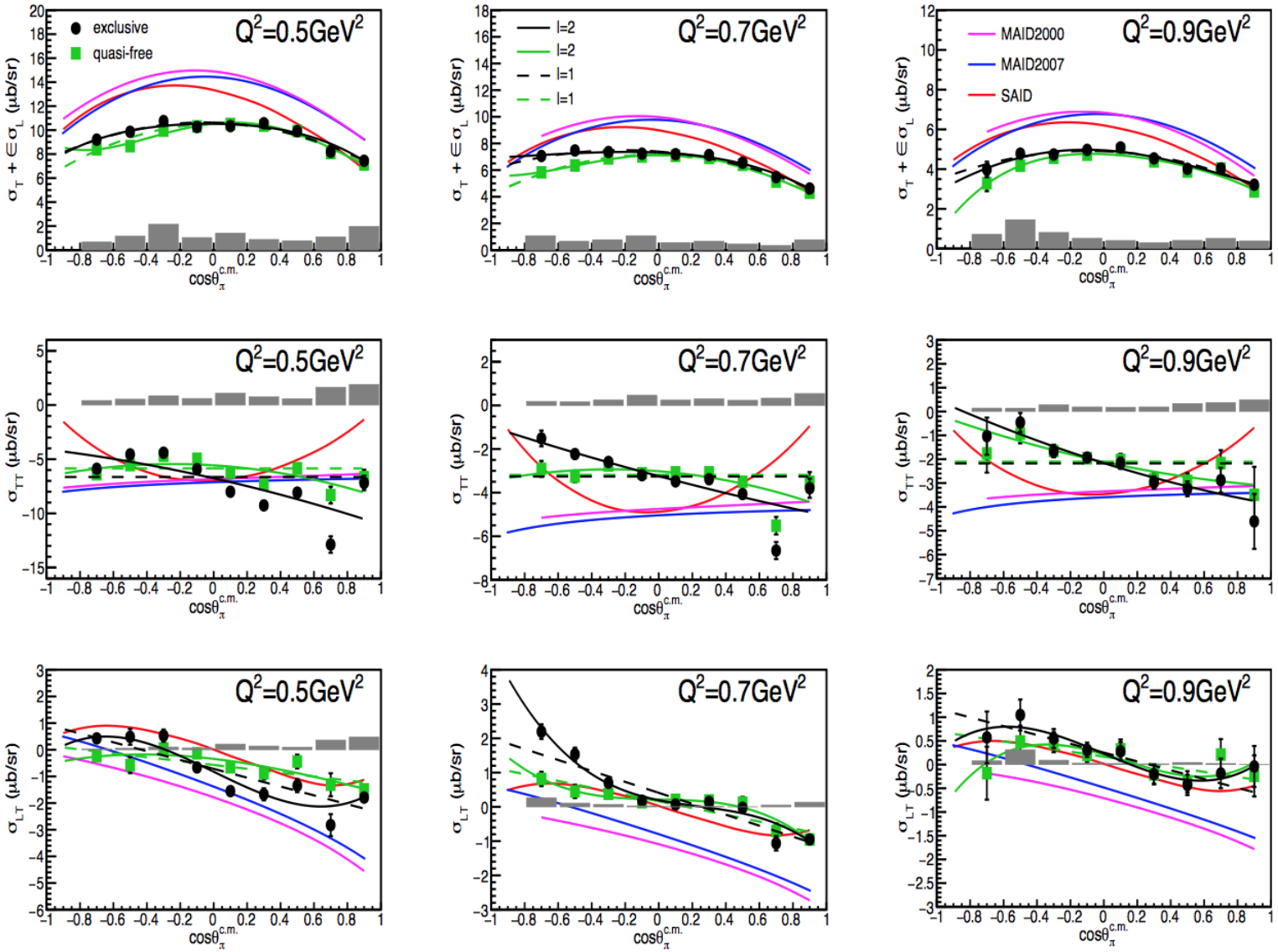
W = 1.6625 GeV



CLAS Database:
https://clasweb.jlab.org/physicsdb/

$\cos\theta_\pi$- Dependent Structure Functions @ W=1.2125 GeV

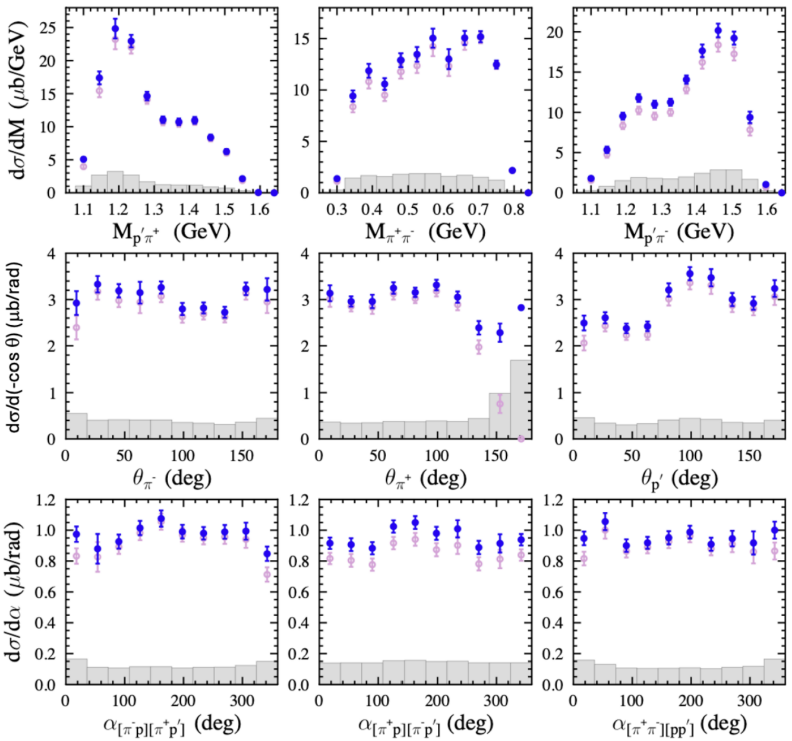
W = 1.2125 GeV ΔW = 25 MeV Ye Tian



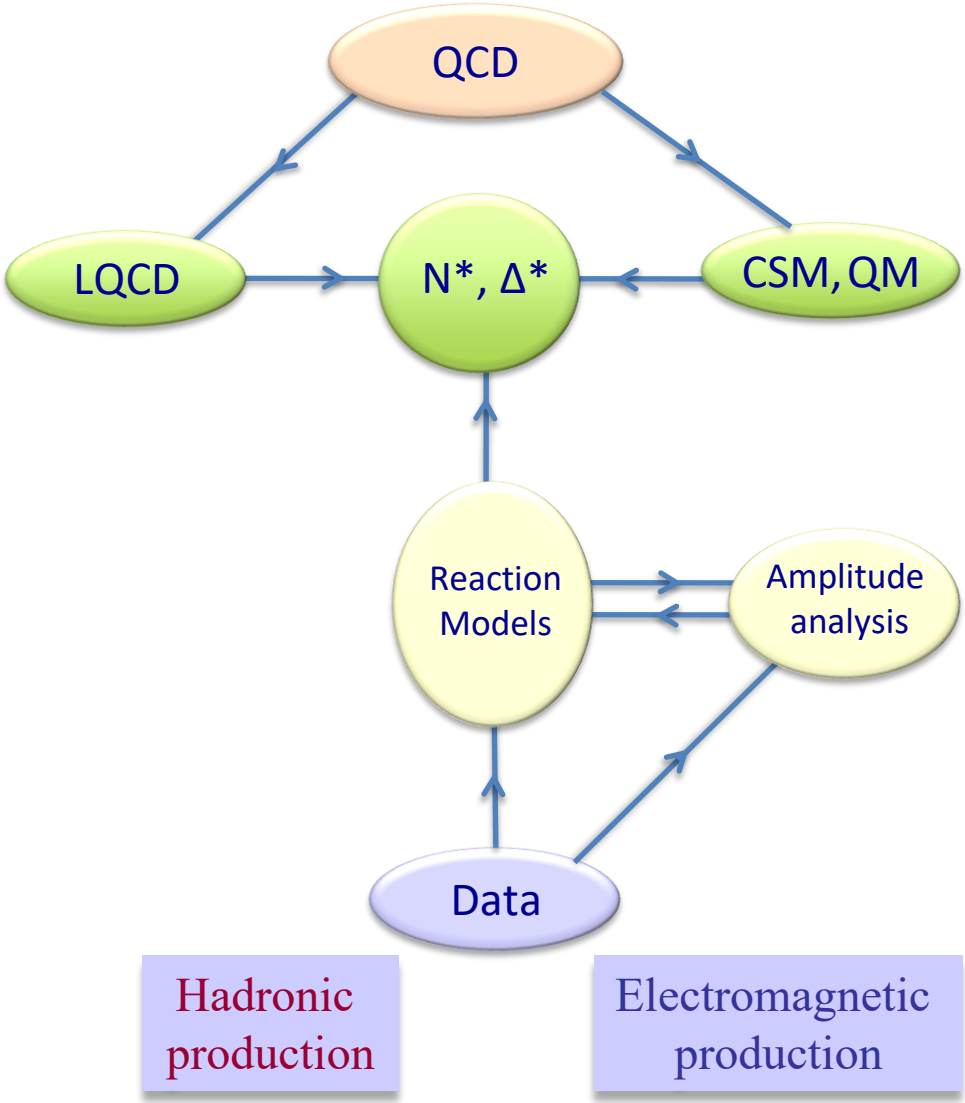
Data-Driven Data Analyses

Consistent Results

Double Pion



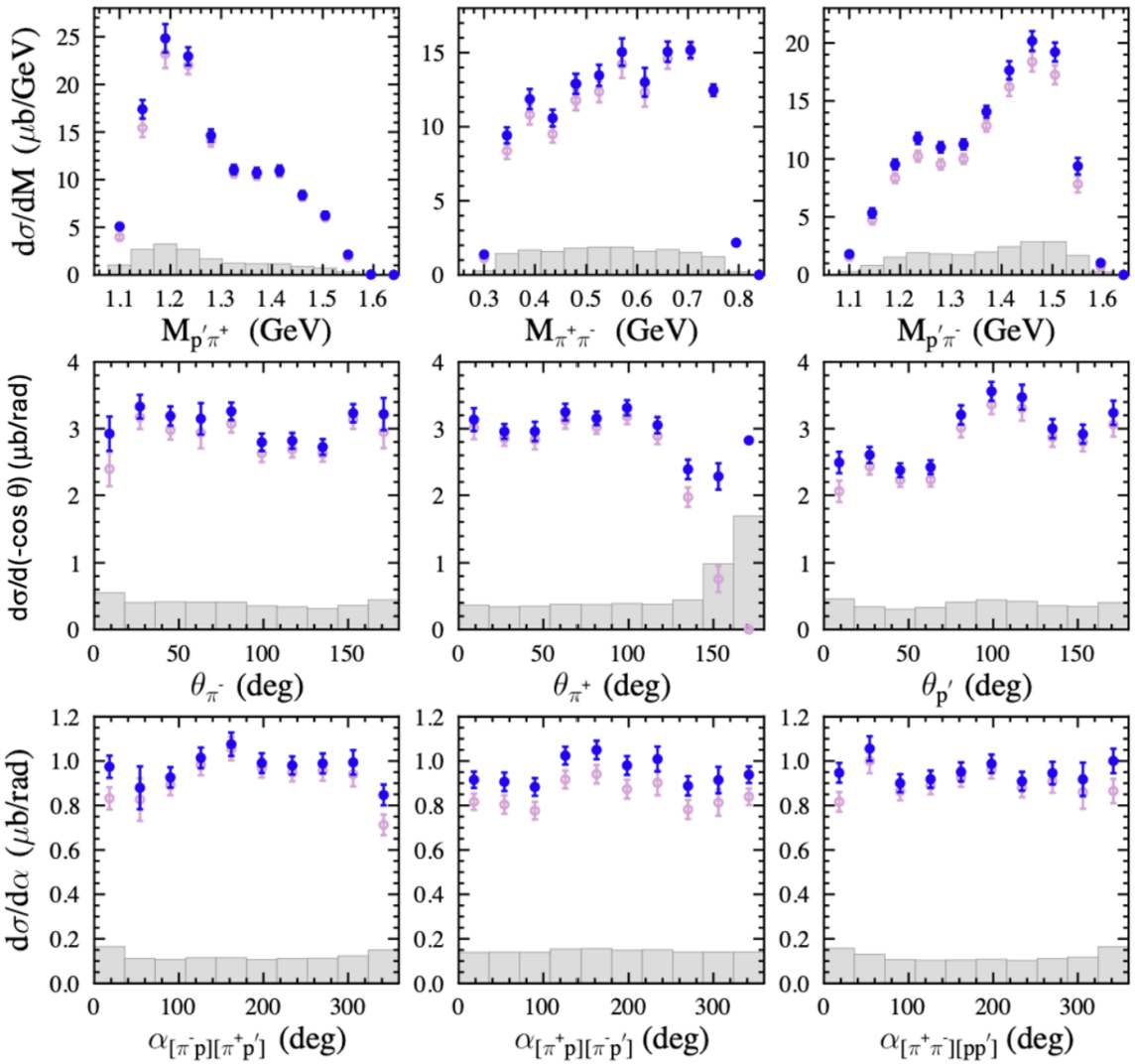
Arjun Trivedi *et al.*, arxiv:2607.06793 (2026)



φ-independent Nππ Single-Differential Cross Sections

Arjun Trivedi

Q^2, W bin $= [2.4, 3.0) GeV^2, [1.725, 1.750) GeV$



final cross sections

without hole filling

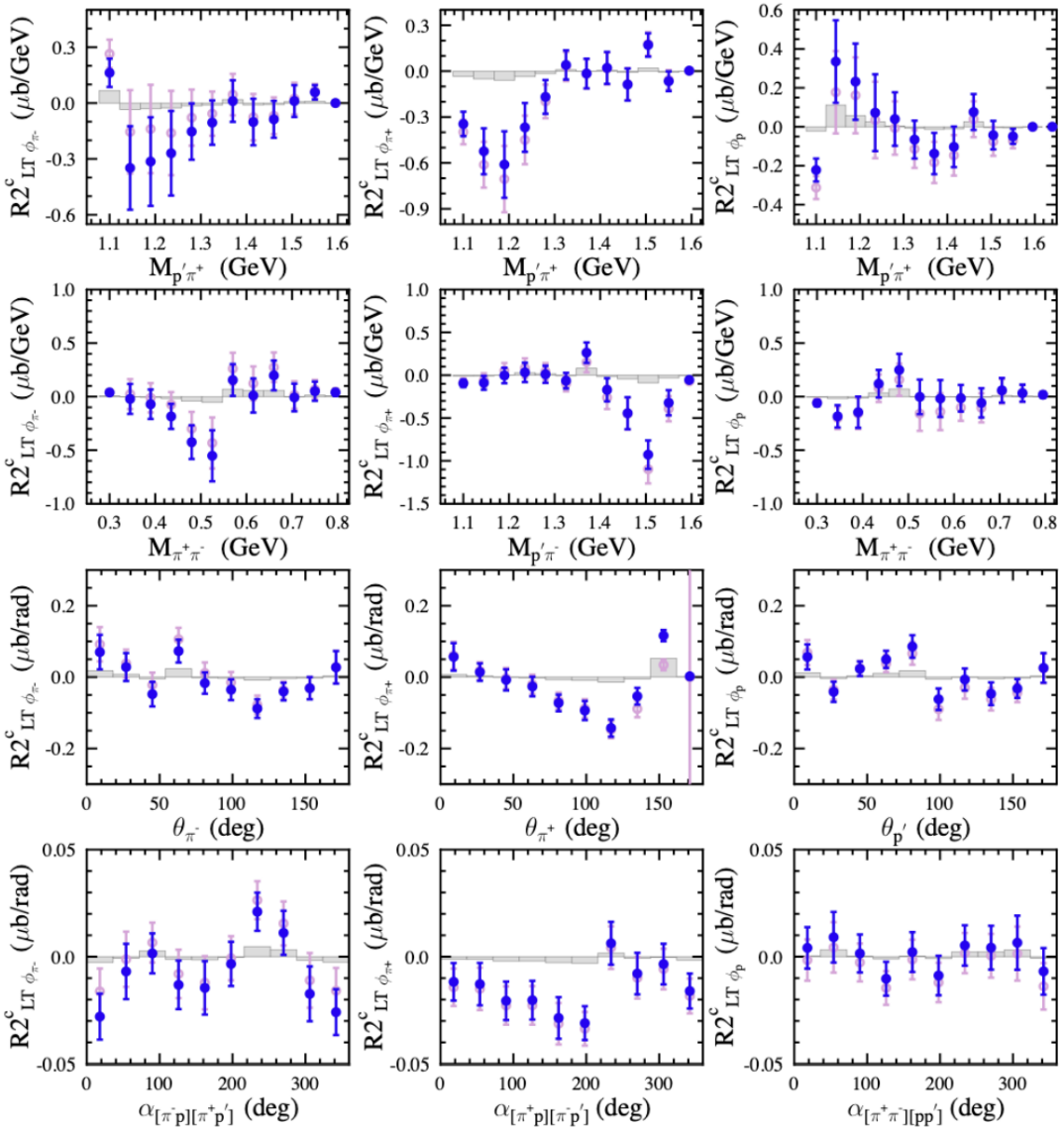
systematic uncertainties

$$\left(\frac{d^2\sigma}{dX_{ij}\,d\phi_i}\right) = R2_T^{X_{ij}} + R2_L^{X_{ij}} + R2_{LT}^{c,X_{ij}} \cos\phi_i + R2_{TT}^{c,X_{ij}} \cos 2\phi_i + \delta_{X_{ij}\alpha_i}\left(R2_{LT}^{s,\alpha_i} \sin\phi_i + R2_{TT}^{s,\alpha_i} \sin 2\phi_i\right)$$

φ-dependent Nππ Single-Differential Cross Sections

Arjun Trivedi

Q^2, W bin $= [2.4, 3.0)GeV^2, [1.725, 1.750)GeV$



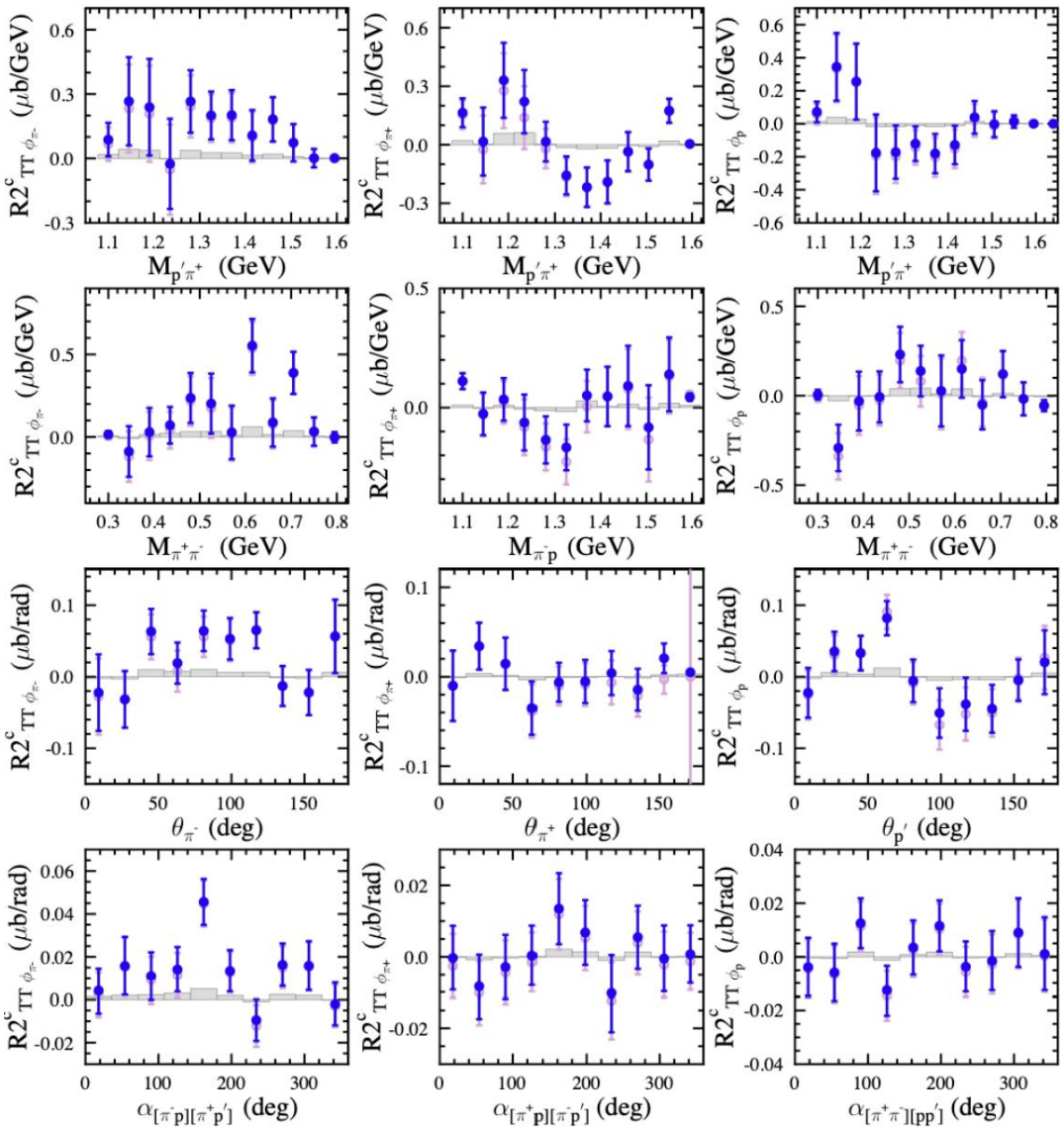
- final cross sections
- without hole filling
- systematic uncertainties

$$\left(\frac{d^2\sigma}{dX_{ij}\,d\phi_i}\right) = R2_T{}^{X_{ij}} + R2_L{}^{X_{ij}} + R2_{LT}{}^{c,X_{ij}}\cos\phi_i + R2_{TT}{}^{c,X_{ij}}\cos 2\phi_i + \delta_{X_{ij}\alpha_i}\left(R2_{LT}{}^{s,\alpha_i}\sin\phi_i + R2_{TT}{}^{s,\alpha_i}\sin 2\phi_i\right)$$

φ-dependent Nππ Single-Differential Cross Sections

Arjun Trivedi

Q^2, W bin $= [2.4, 3.0)\,GeV^2, [1.725, 1.750)\,GeV$



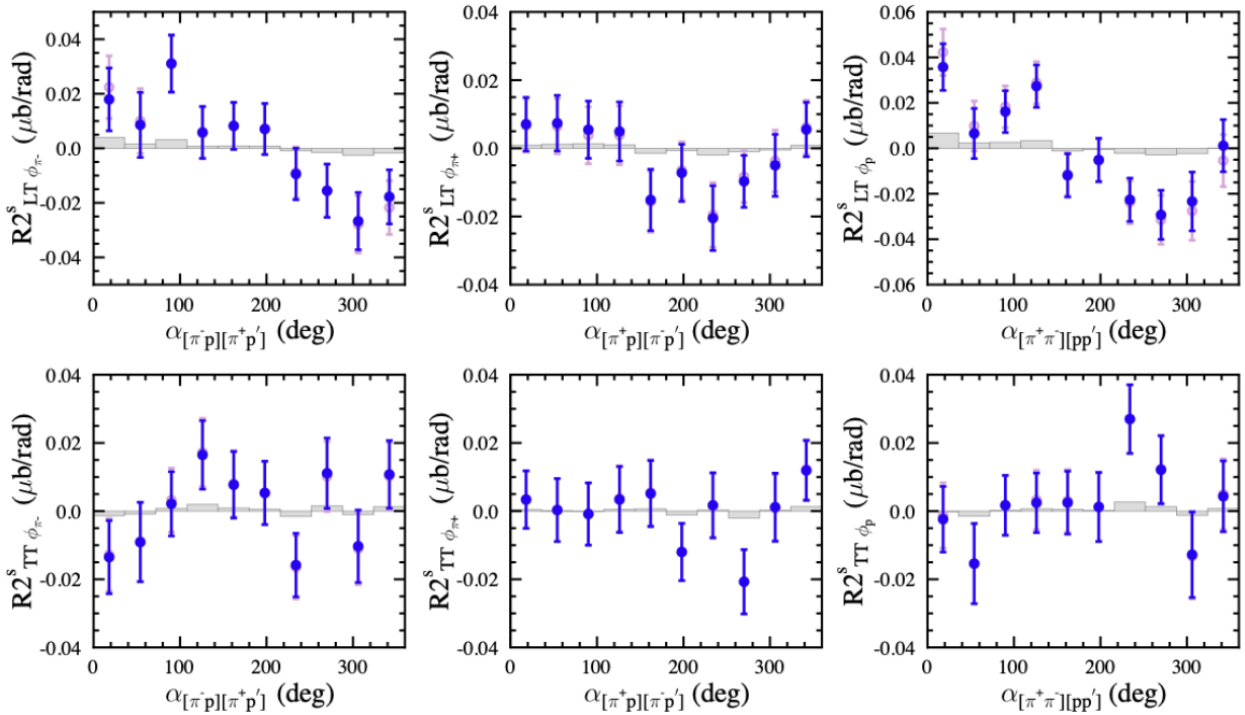
- final cross sections
- without hole filling
- systematic uncertainties

$$\left(\frac{d^2\sigma}{dX_{ij}\,d\phi_i}\right) = R2_T{}^{X_{ij}} + R2_L{}^{X_{ij}} + R2_{LT}{}^{c,X_{ij}}\cos\phi_i + R2_{TT}{}^{c,X_{ij}}\cos 2\phi_i + \delta_{X_{ij}\alpha_i}\left(R2_{LT}{}^{s,\alpha_i}\sin\phi_i + R2_{TT}{}^{s,\alpha_i}\sin 2\phi_i\right)$$

φ-dependent Nππ Single-Differential Cross Sections

Arjun Trivedi

Q^2, W bin $= [2.4, 3.0)GeV^2, [1.725, 1.750)GeV$

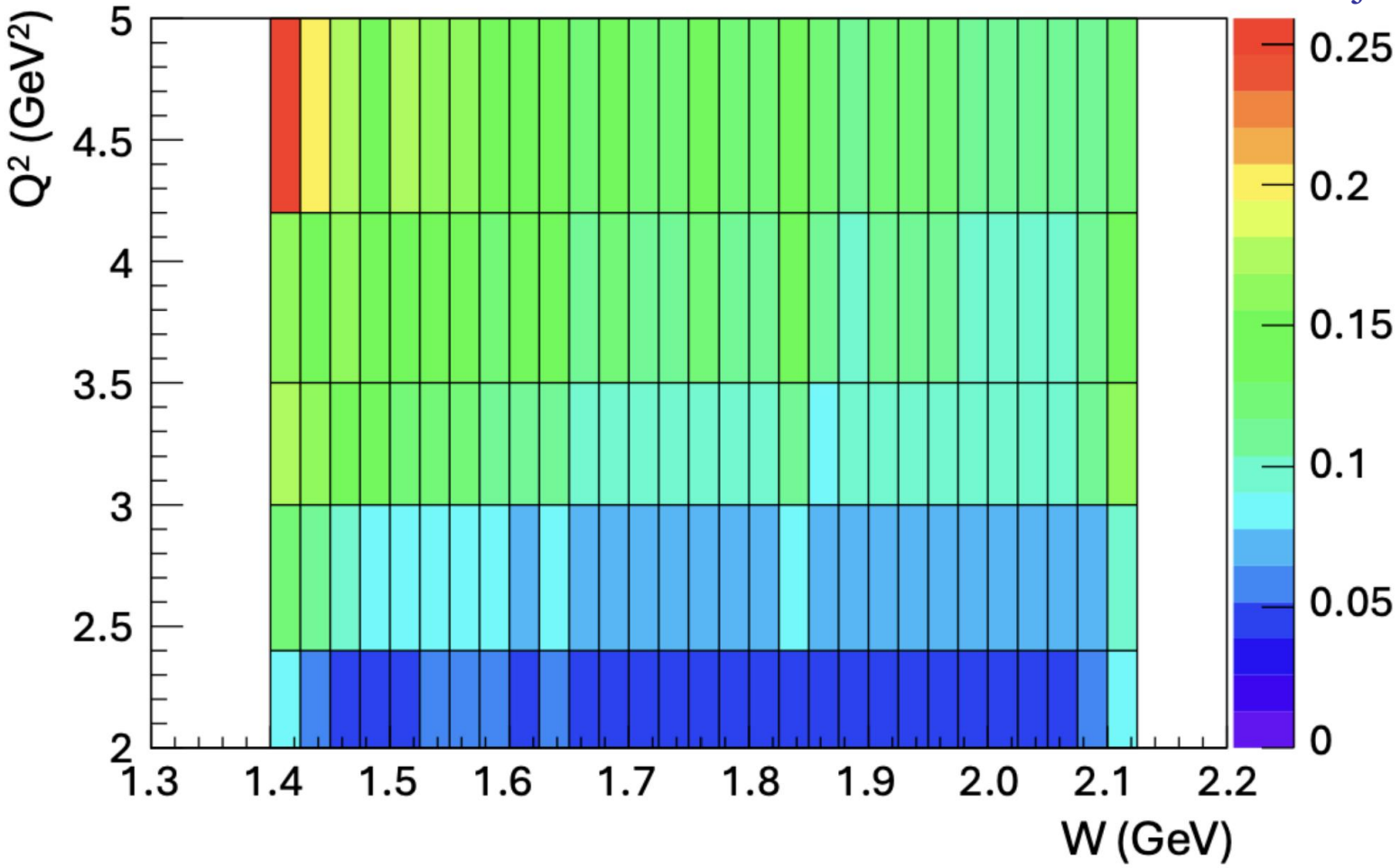


A. Trivedi, under PRC review, arXiv:2607.06793v2

$$\left(\frac{d^2\sigma}{dX_{ij}d\phi_i}\right) = R2_T{}^{X_{ij}} + R2_L{}^{X_{ij}} + R2_{LT}{}^{c,X_{ij}}\cos\phi_i + R2_{TT}{}^{c,X_{ij}}\cos 2\phi_i + \delta_{X_{ij}\alpha_i}\left(R2_{LT}{}^{s,\alpha_i}\sin\phi_i + R2_{TT}{}^{s,\alpha_i}\sin 2\phi_i\right)$$

Acceptance Averaged over Hadronic Phase Space

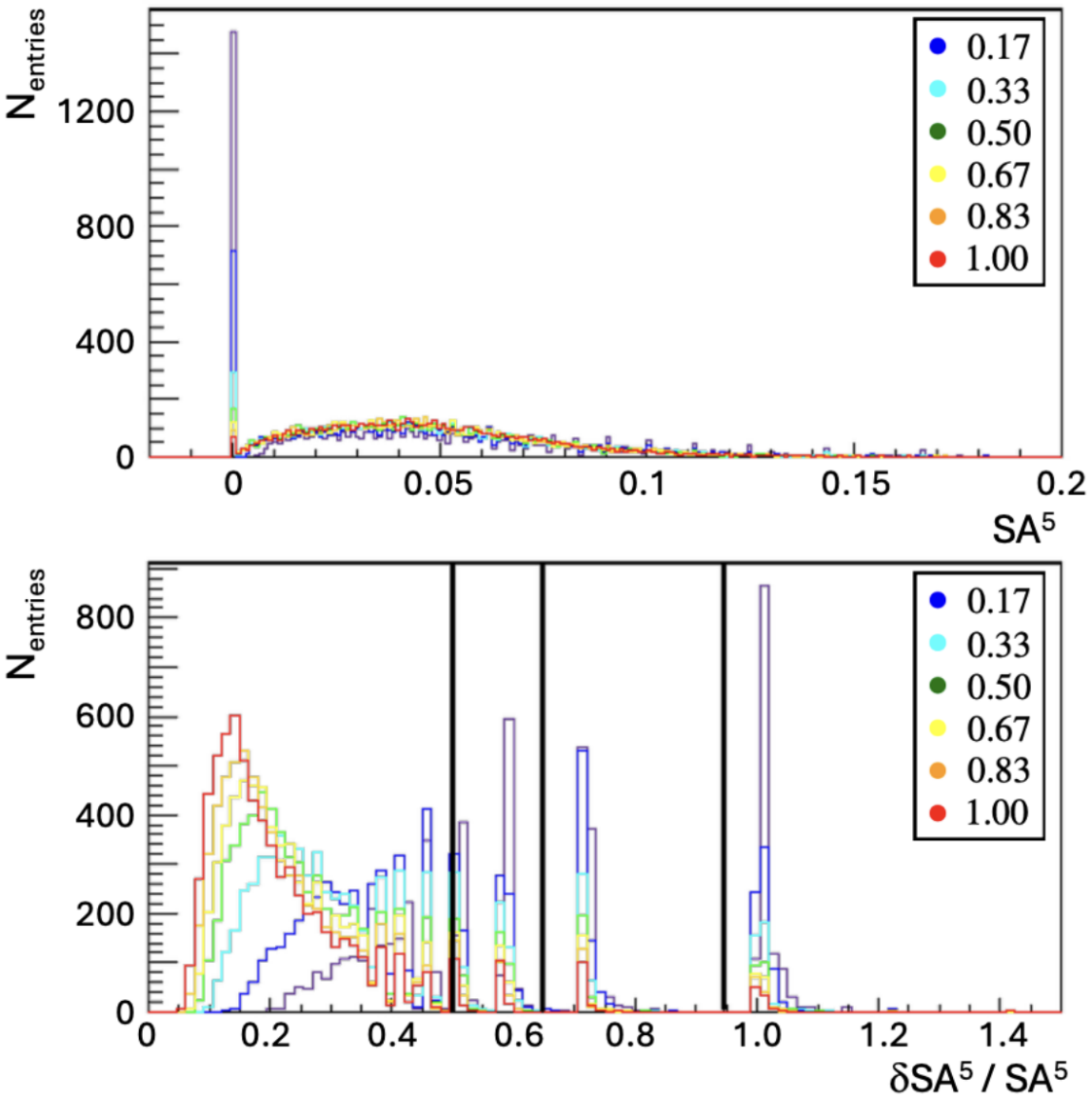
Arjun Trivedi



Although we have only 145 2D phase space cells (W,Q^2), the number of kinematically independent 5D PSCs is 196,000, which leads to a total number of PSCs of 29,420,000.

Acceptance and Acceptance Error Cuts

Arjun Trivedi



Zero acceptance cells

- No reconstructed events
- No thrown events

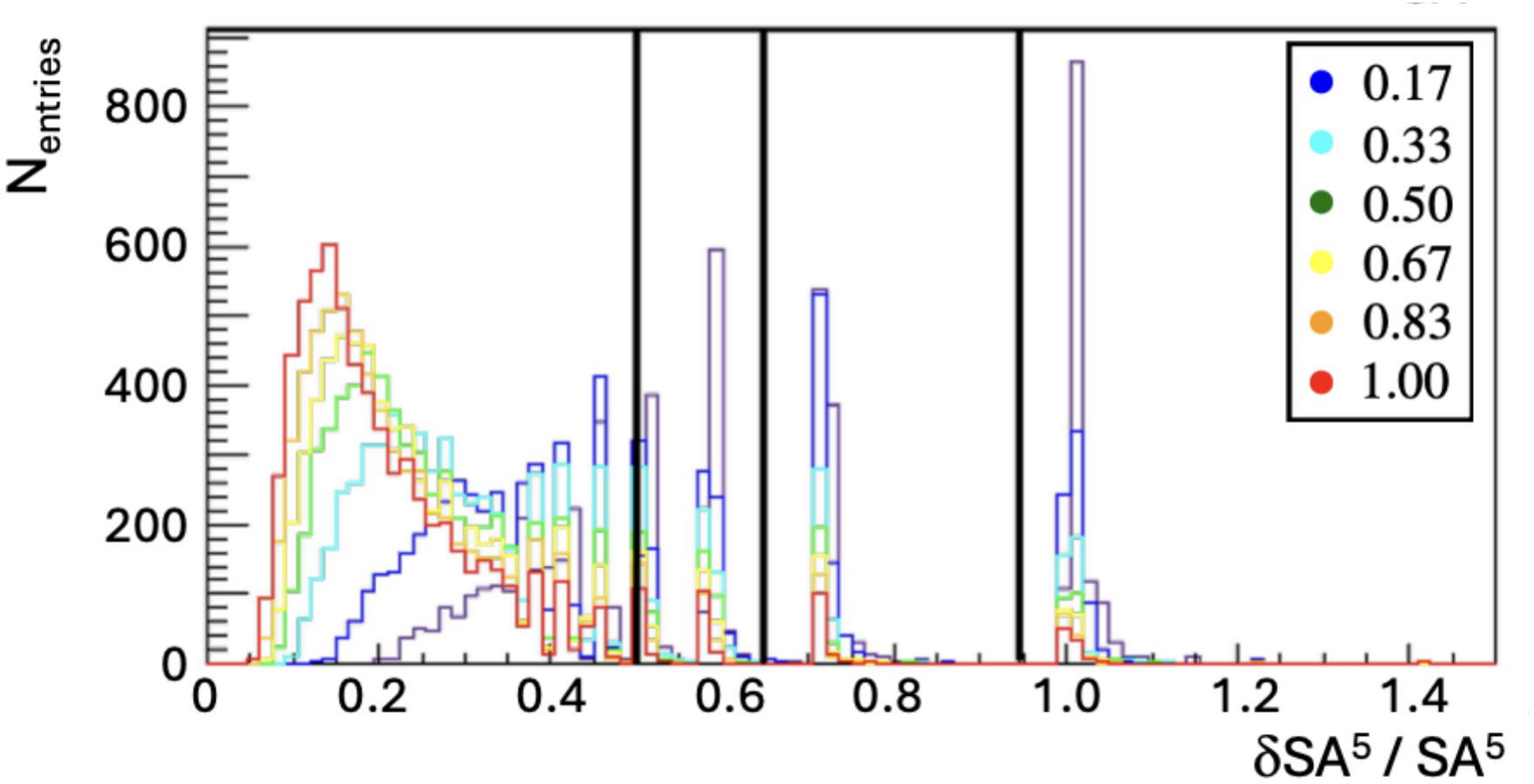
Large acceptance errors

- Few reconstructed events
- Avoid infinite simulation
- Avoid Poisson error bars

Acceptance and Acceptance Error Cuts

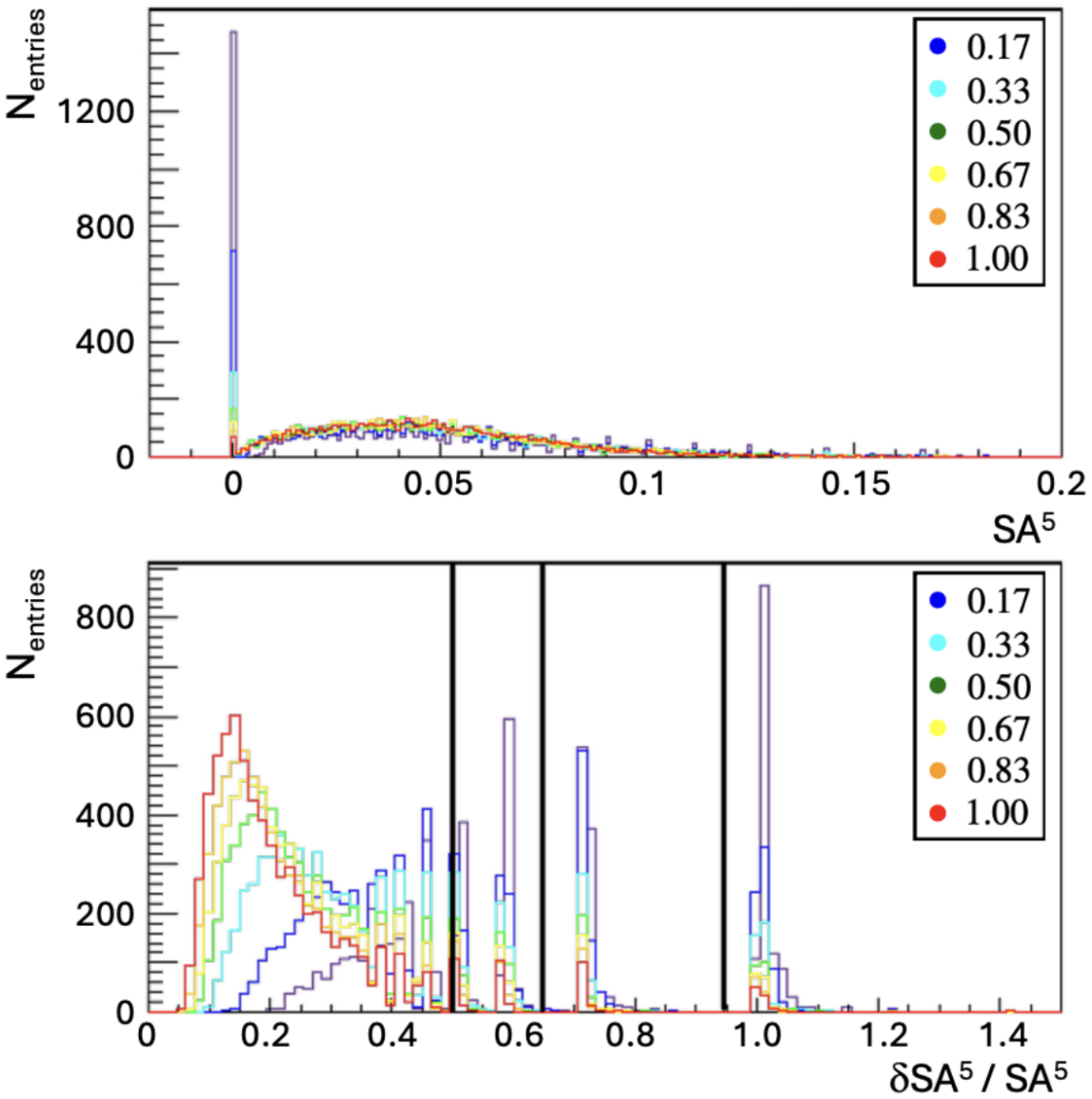
Arjun Trivedi

[2.00, 2.40] GeV^2, W = [1.650, 1.675] GeV



Acceptance and Acceptance Error Cuts

Arjun Trivedi



Zero acceptance cells

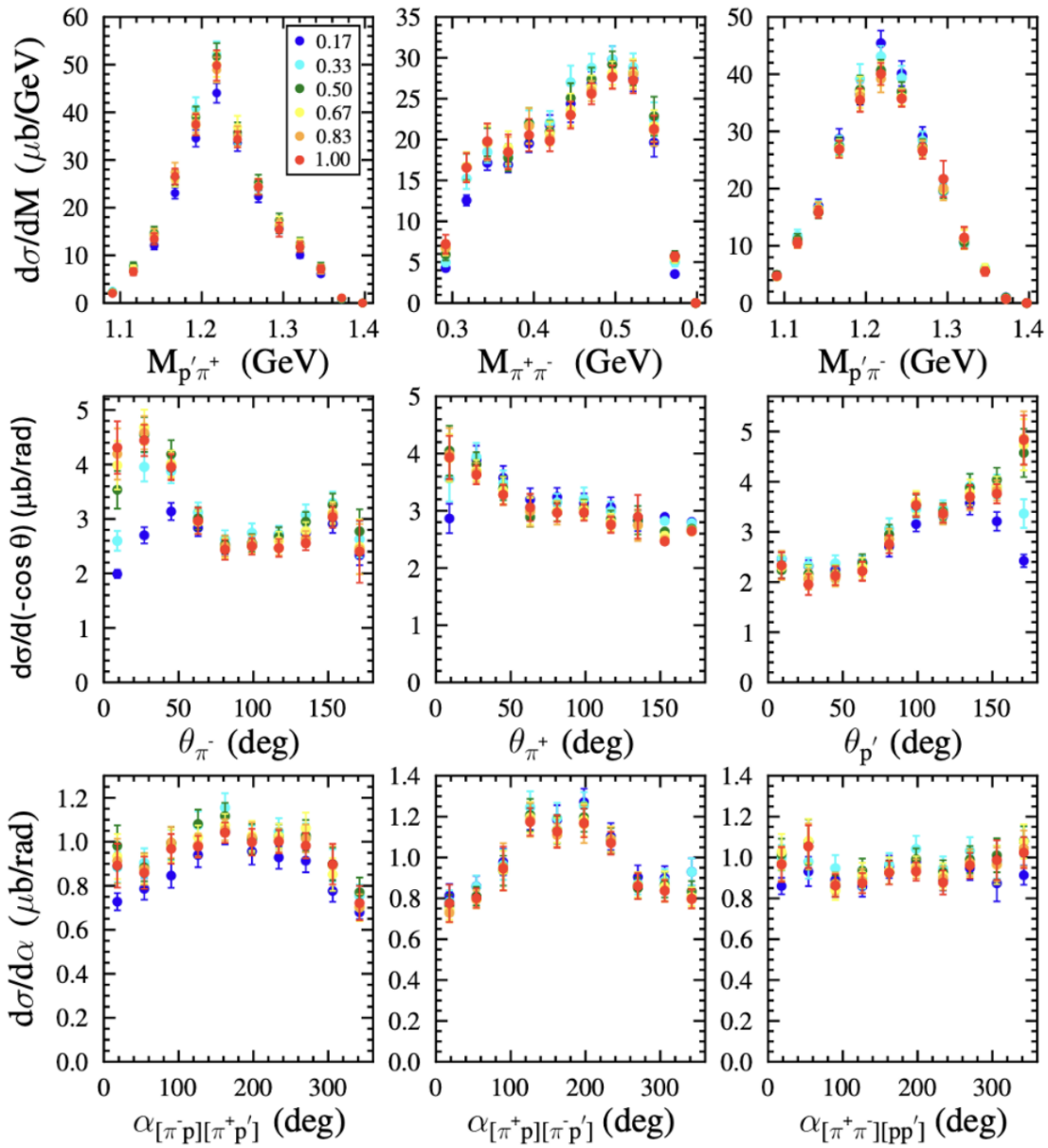
- No reconstructed events
- No thrown events

Large acceptance errors

- Few reconstructed events
- Avoid infinite simulation
- Avoid Poisson error bars

Acceptance and Acceptance Error Cuts

Arjun Trivedi



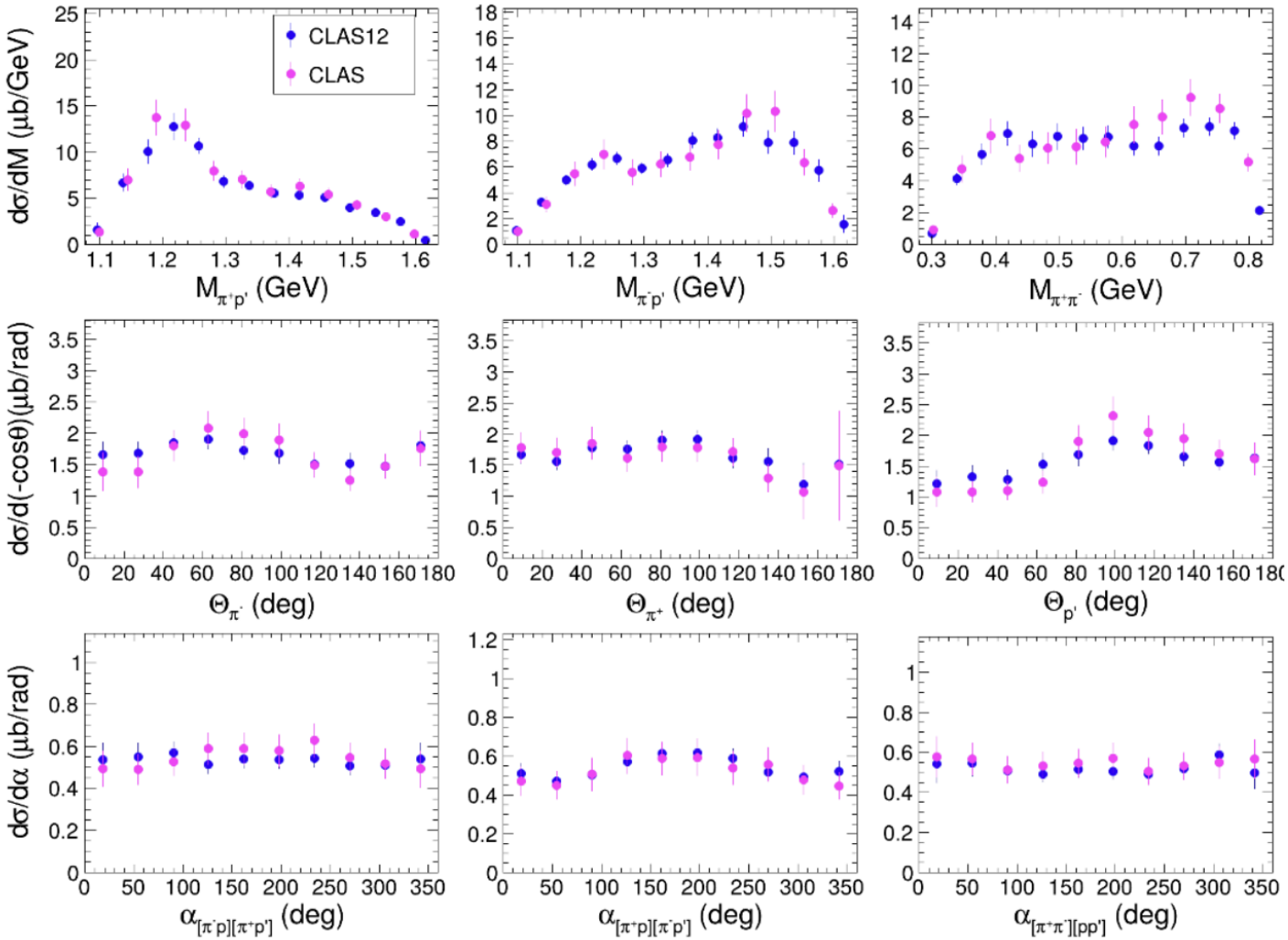
Cross section errors

- Optimize stability
- Symmetric fluctuations
- Symmetric error bars
- Minimize systematic errors

Nππ Single-Differential Cross Sections

W ∈ [1.75, 1.80] GeV and Q^2 ∈ [3.0, 3.5] GeV^2

Krishna Neupane
Arjun Trivedi



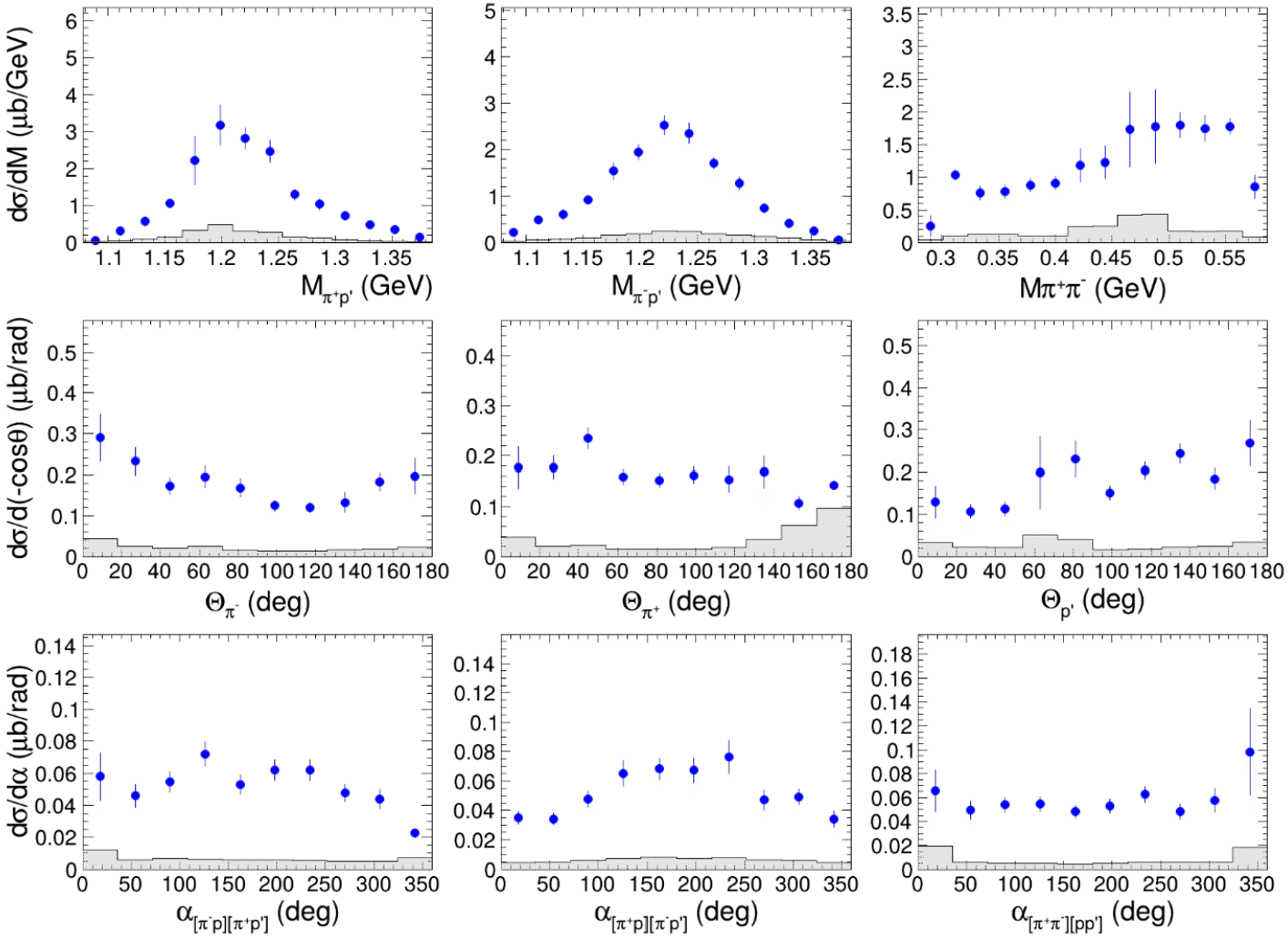
- Krishna
  arXiv:2609.19395v2
- Arjun
  arXiv:2607.06793v2

$$\left(\frac{d^2\sigma}{dX_{ij}\,d\phi_i}\right) = R2_T^{X_{ij}} + R2_L^{X_{ij}} + R2_{LT}^{c,X_{ij}}\cos\phi_i + R2_{TT}^{c,X_{ij}}\cos 2\phi_i + \delta_{X_{ij}\alpha_i}\left(R2_{LT}^{s,\alpha_i}\sin\phi_i + R2_{TT}^{s,\alpha_i}\sin 2\phi_i\right)$$

Nππ Single-Differential Cross Sections

W ∈ [1.50, 1.55] GeV and Q^2 ∈ [6.0, 7.0] GeV^2

Krishna Neupane



- final cross sections
- systematic uncertainties

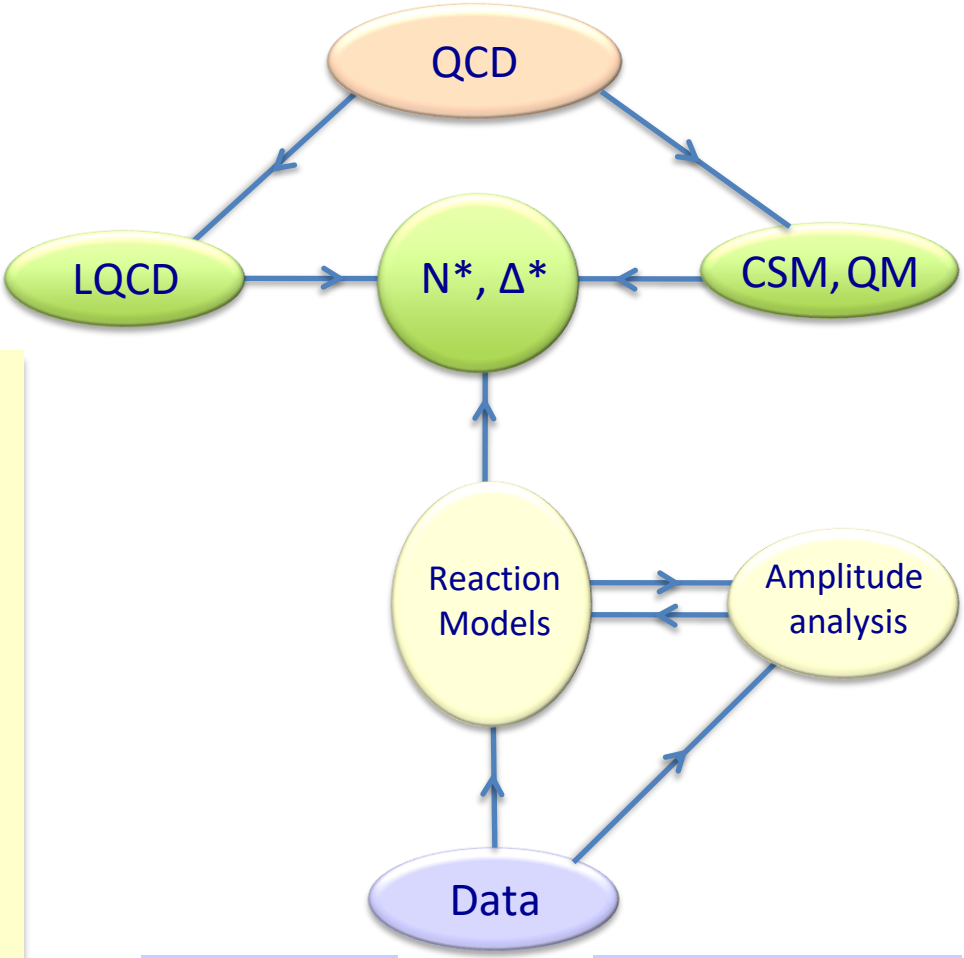
Krishna (Friday)

$$\left(\frac{d^2\sigma}{dX_{ij}\,d\phi_i}\right) = R2_T^{X_{ij}} + R2_L^{X_{ij}} + R2_{LT}^{c,X_{ij}}\cos\phi_i + R2_{TT}^{c,X_{ij}}\cos 2\phi_i + \delta_{X_{ij}\alpha_i}\left(R2_{LT}^{s,\alpha_i}\sin\phi_i + R2_{TT}^{s,\alpha_i}\sin 2\phi_i\right)$$

Phenomenological Analysis

Data-Driven Data Analyses

Consistent Results

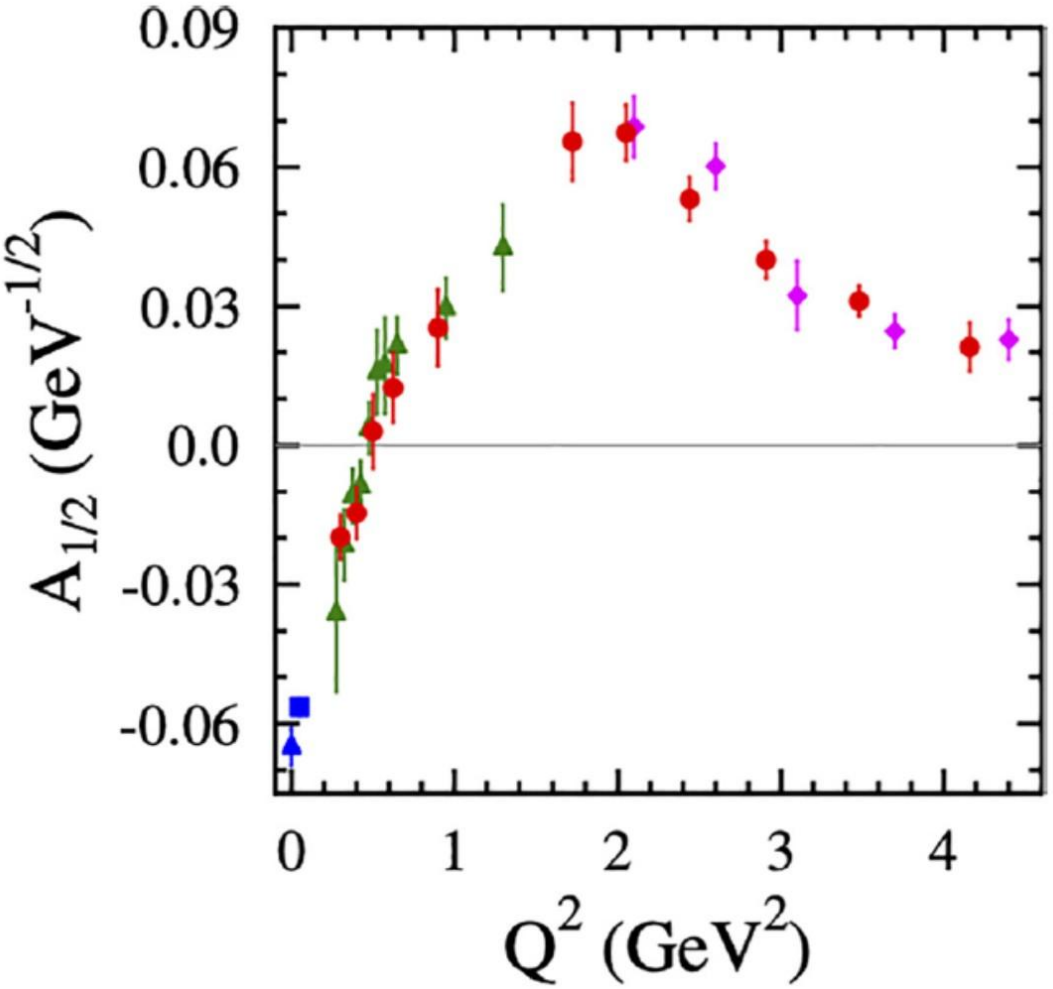


- Single meson production:
  - Unitary Isobar Model (JANR, MAID, SAID)
  - Fixed-*t* Dispersion Relations (JANR)
- Double pion production:
  - Unitarized Isobar Model (JM)
- Coupled-Channel Approaches:
  - EBAC ⇒ Argonne-Osaka
  - JBW ⇒ Jülich-Bonn-Washington
  - BoGa ⇒ Bonn-Gatchina

Int. J. Mod. Phys. E, Vol. 22, 1330015 (2013) 1-99

N(1440)1/2$^+$ Couplings from CLAS

Viktor Mokeev

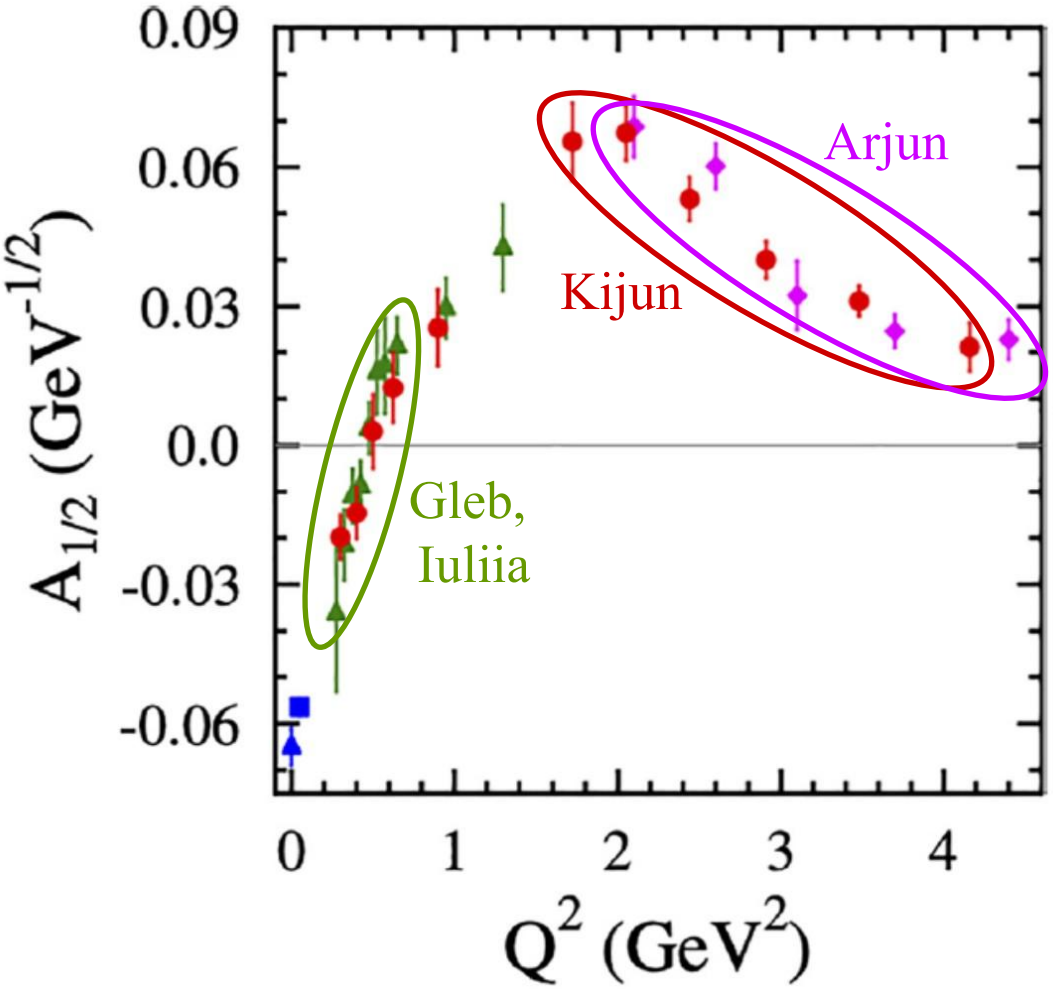


Consistent results are now obtained in the low-lying resonance region up to a Q^2 of 5 GeV^2 by independent analyses from the Nπ differential cross sections, beam, target, and beam-target asymmetries (red bullets, left) and p$\pi^+\pi^-$ differential cross sections (purple diamonds, green triangles). All observables have fundamentally different mechanisms for the nonresonant background and underscore the capability of the reaction models to extract reliable resonance electrocouplings.

V. Mokeev *et al.*, Phys. Rev. C 108, 025204 (2023) 1-26

N(1440)1/2$^+$ Couplings from CLAS

Viktor Mokeev

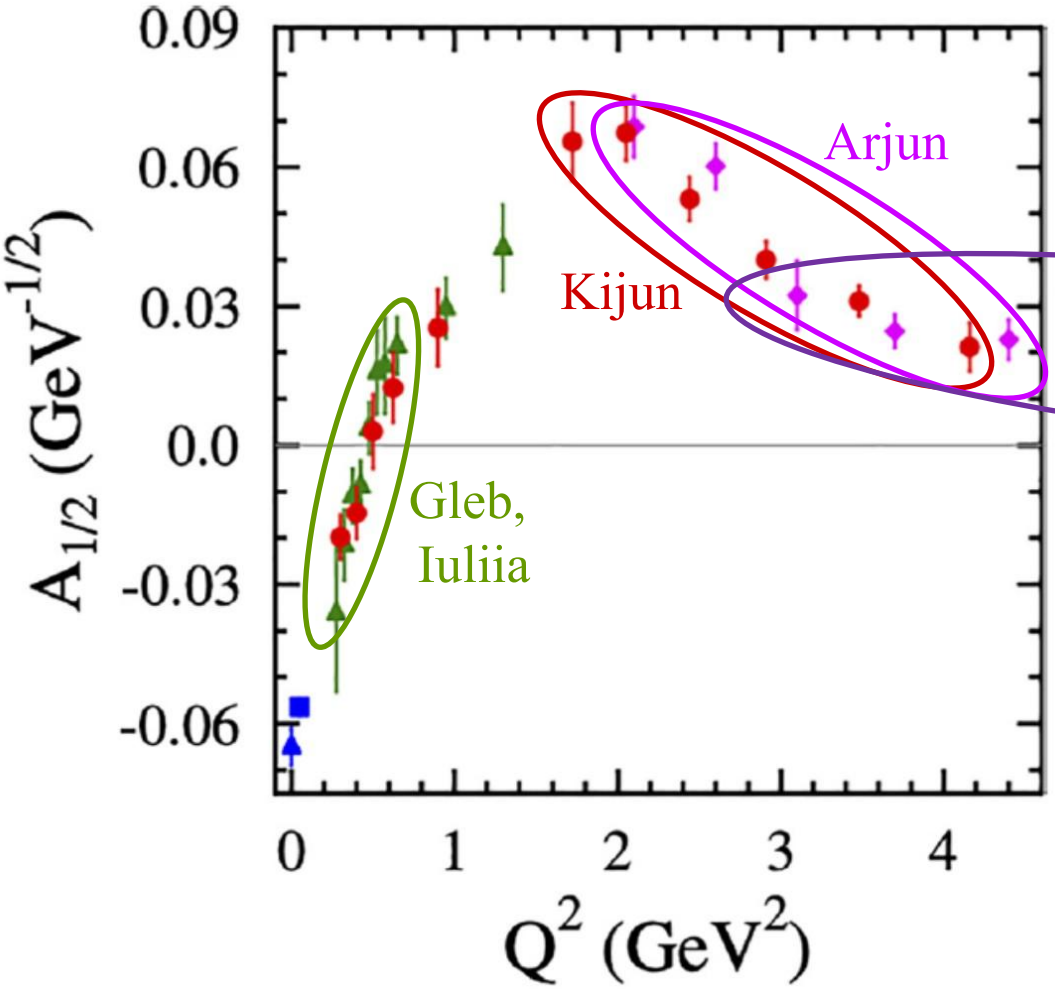


Consistent results are now obtained in the low-lying resonance region up to a Q^2 of 5 GeV^2 by independent analyses from the $N\pi$ differential cross sections, beam, target, and beam-target asymmetries (red bullets, left) and $p\pi^+\pi^-$ differential cross sections (purple diamonds, green triangles). All observables have fundamentally different mechanisms for the nonresonant background and underscore the capability of the reaction models to extract reliable resonance electrocouplings.

V. Mokeev *et al.*, Phys. Rev. C 108, 025204 (2023) 1-26

N(1440)1/2$^+$ Couplings from CLAS

Viktor Mokeev



Arjun

Kijun

CLAS12

Gleb, Iuliia

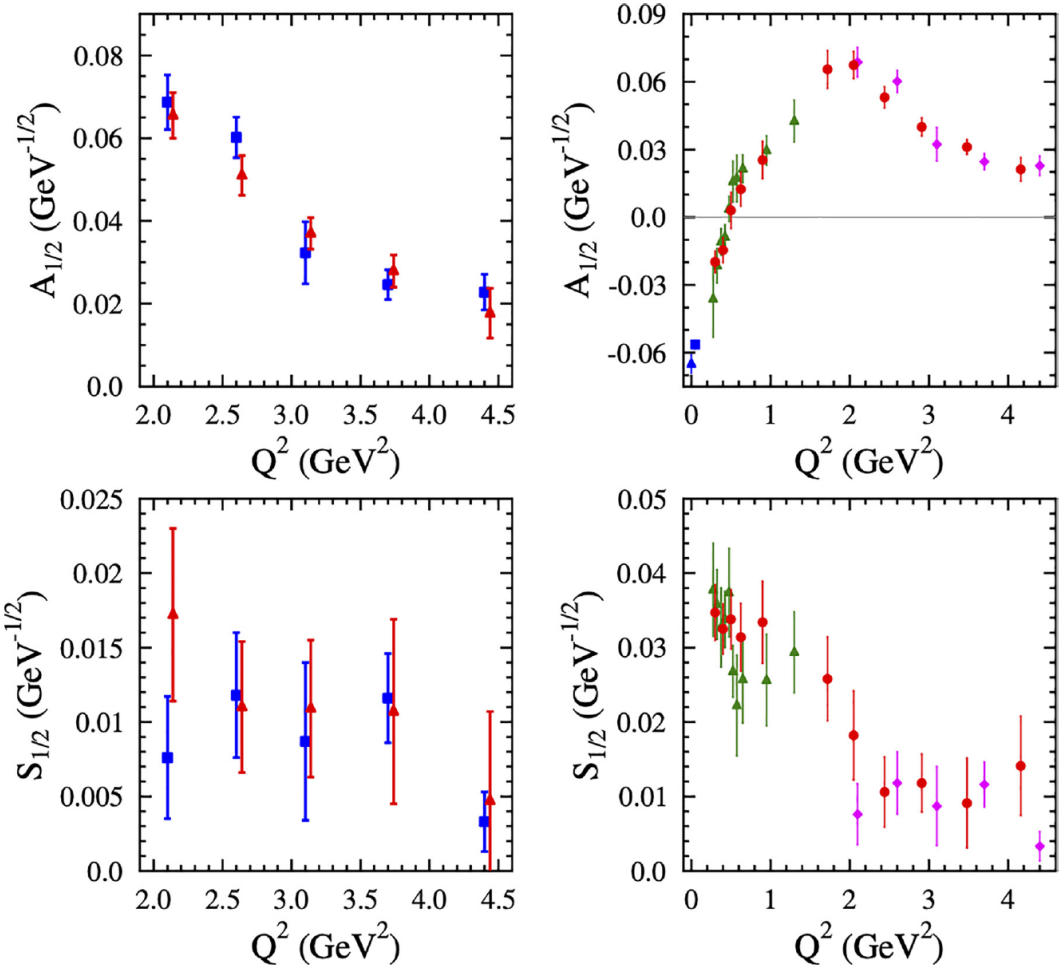
Krishna, Alexis

USC Cross Sections

V. Mokeev *et al.*, Phys. Rev. C 108, 025204 (2023) 1-26 and http://arxiv.org/abs/2608.04997

N(1440)1/2$^+$ Couplings from CLAS

Viktor Mokeev

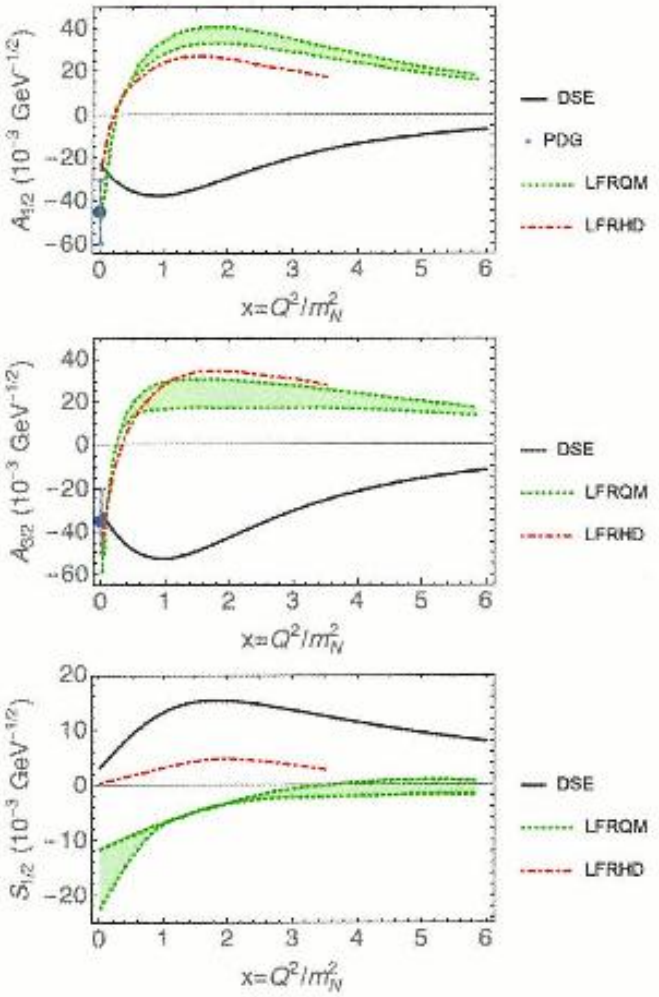


Consistent results are now obtained in the low-lying resonance region up to a Q^2 of 5 GeV^2 by independent analyses from the $N\pi$ differential cross sections, beam, target, and beam-target asymmetries (red triangles, left) and $p\pi^+\pi^-$ differential cross sections (blue squares, left). All observables have fundamentally different mechanisms for the nonresonant background and underscore the capability of the reaction models to extract reliable resonance electrocouplings.

V. Mokeev *et al.*, Phys. Rev. C 108, 025204 (2023) 1-26

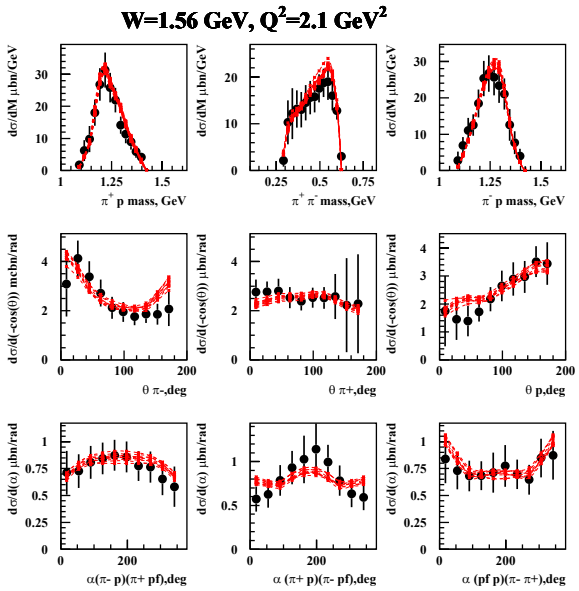
$\Delta(1600)3/2^+$ Form Factors in CSM Approach

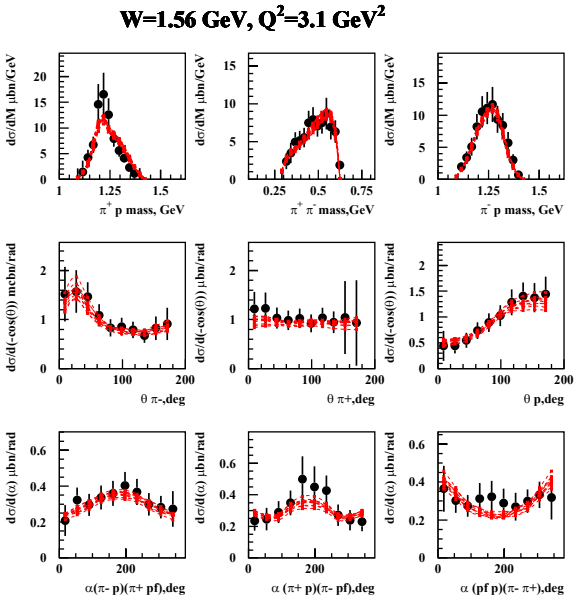
CSM predictions of the $\Delta(1600)3/2^+$ electrocouplings



Ya Lu et al., PRD 100, 034001 (2019)

Arjun Trivedi
Viktor Mokeev

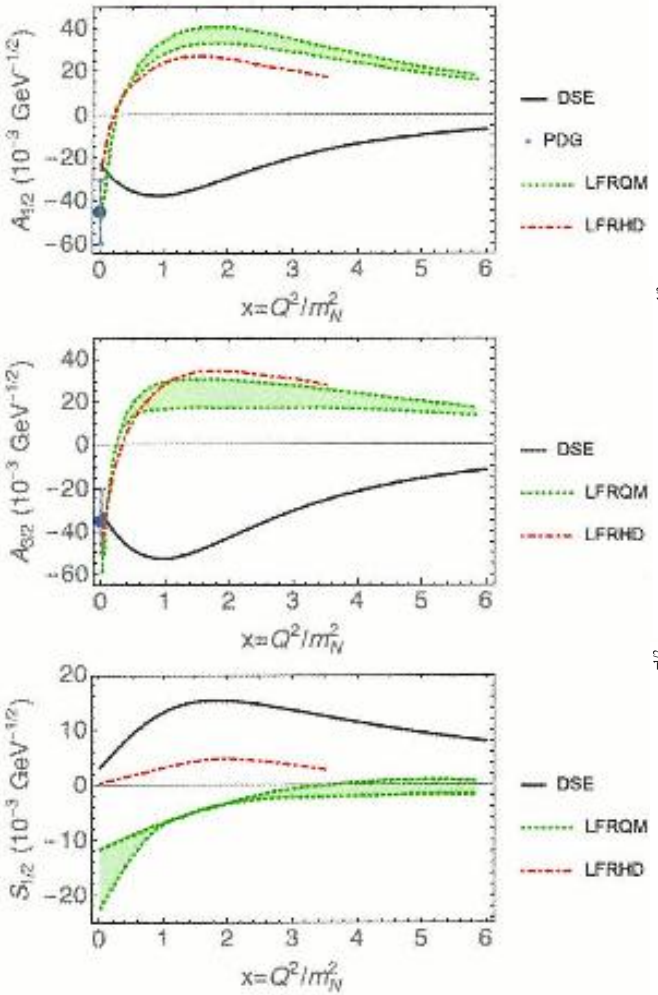


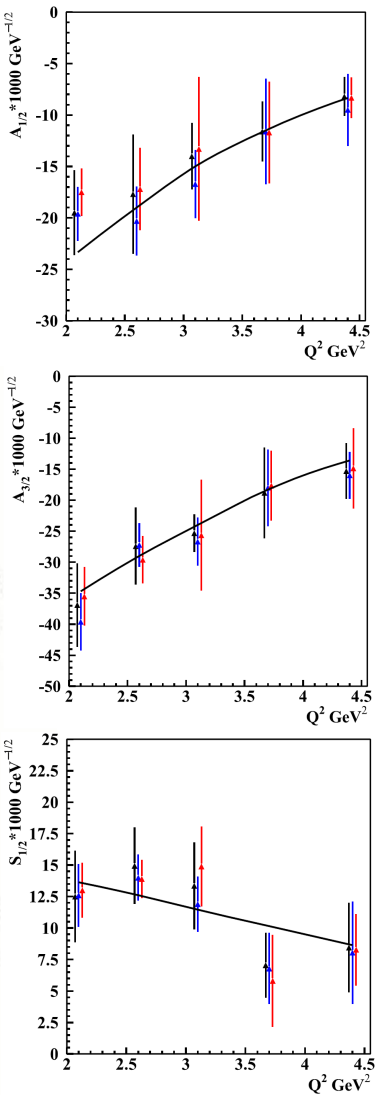


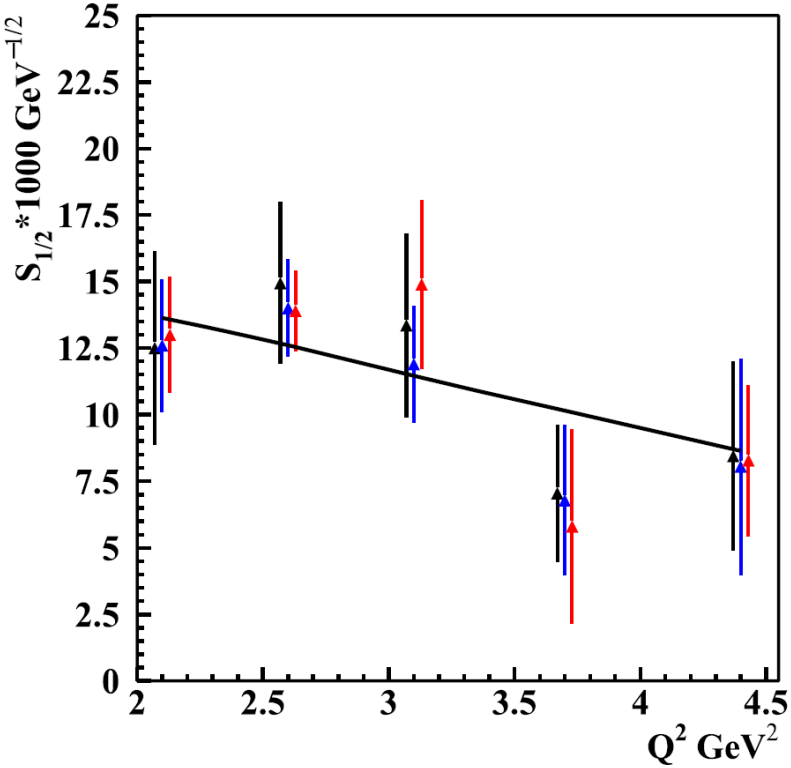
$\Delta(1600)3/2^+$ Form Factors in CSM Approach

Viktor Mokeev

CSM predictions of the $\Delta(1600)3/2^+$ electrocouplings







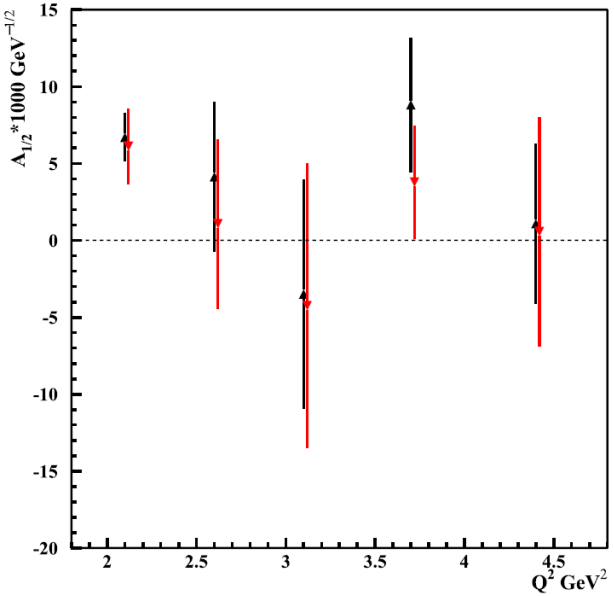
JM analysis of Arjun's $\pi^+\pi^-p$ differential cross sections for $2.0\text{GeV}^2<Q^2<5.0\text{GeV}^2$ within $1.56\text{GeV}<W<1.66\text{GeV}$ and $1.61\text{GeV}<W<1.71\text{GeV}$ with varied compared to previously fixed hadronic parameter for $M_{N^*}>1.65$.

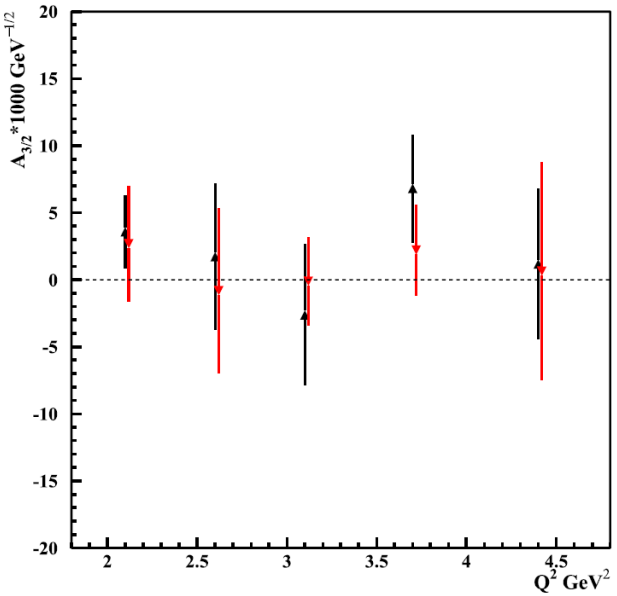
Ya Lu et al., PRD 100, 034001 (2019)

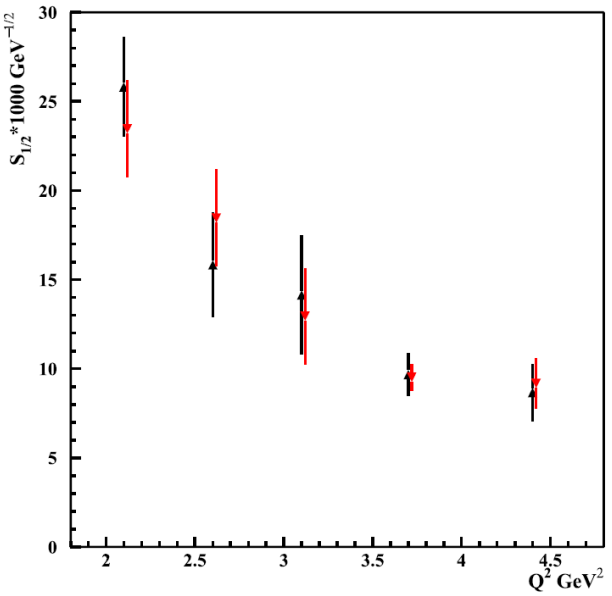
Phys. Rev. C 108, 025204 (2023) 1-26

$\Delta(1700)3/2^-$ Couplings from CLAS

Viktor Mokeev







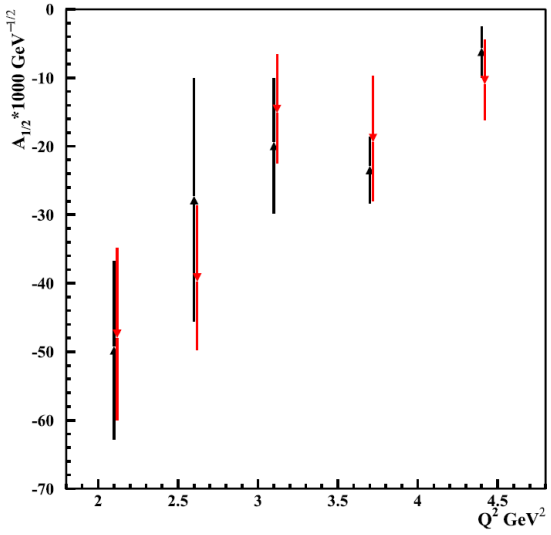
JM23 analysis of Arjun's $\pi^+\pi^-p$ differential cross sections for $2.0\text{GeV}^2<Q^2<5.0\text{GeV}^2$ within $1.61\text{GeV}<W<1.71\text{GeV}$ and $1.66\text{GeV}<W<1.76\text{GeV}$.

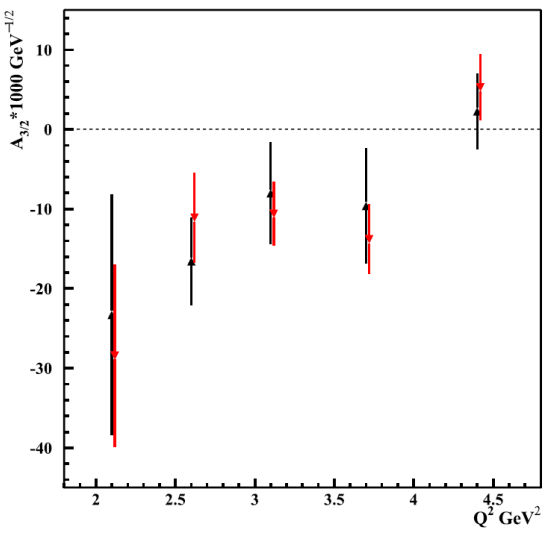
$\Delta(1700)3/2^-$ chiral partner of $\Delta(1232)3/2^+$

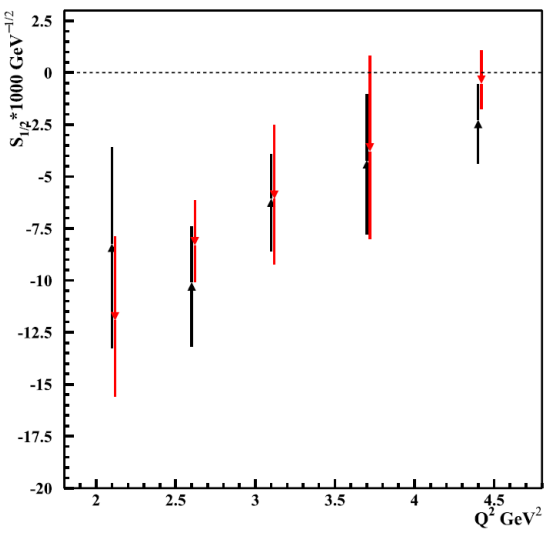
V. Mokeev *et al.*, under PRC review, http://arxiv.org/abs/2608.04997

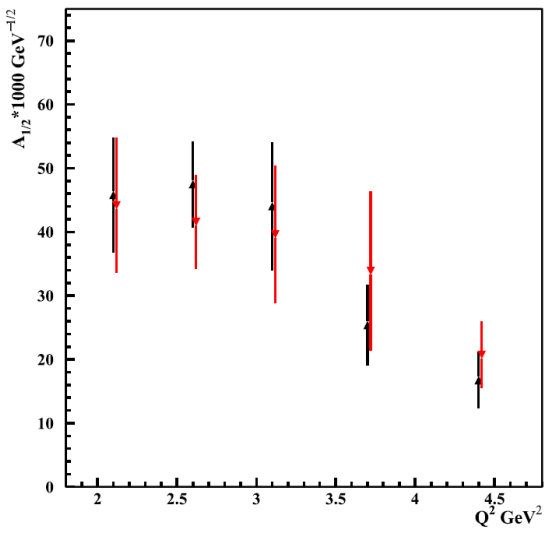
N(1720)3/2$^+$ and N'(1720)3/2$^+$ Couplings from CLAS

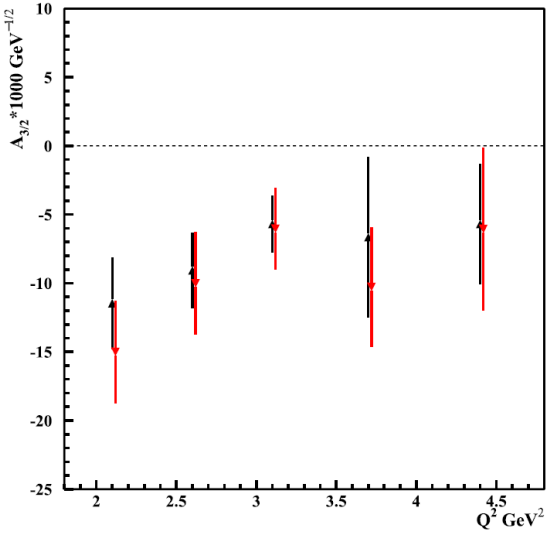
Viktor Mokeev

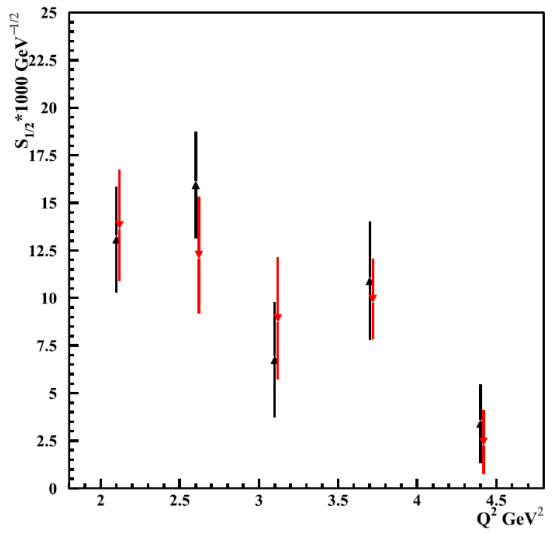








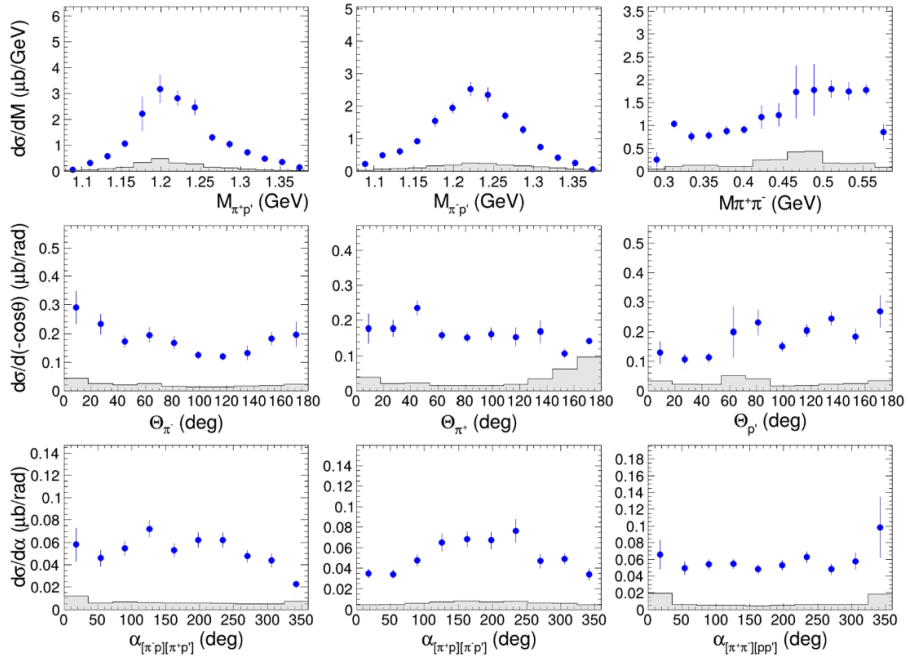




JM23 analysis of Arjun's $\pi^+\pi^-$p differential cross sections for 2.0GeV^2<Q^2<5.0GeV^2 within 1.61GeV<W<1.71GeV and 1.66GeV<W<1.76GeV with consistent hadronic parameters when compared to PL B805, 135457 (2020).

Conclusion

Emergence of Hadron Mass and Structure

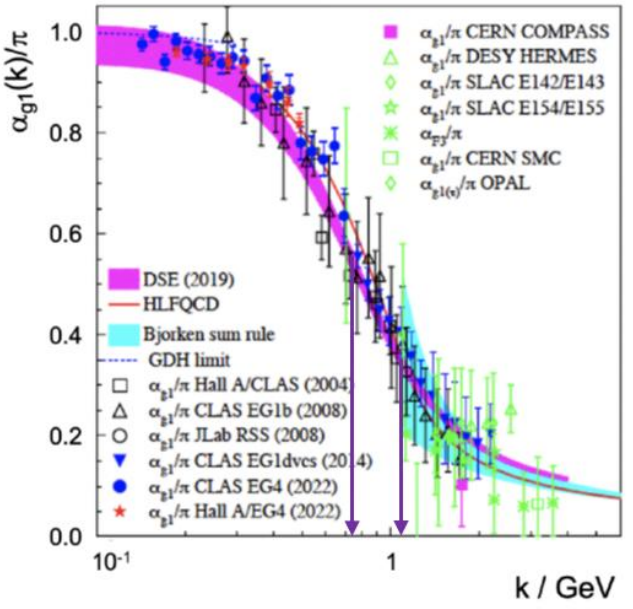


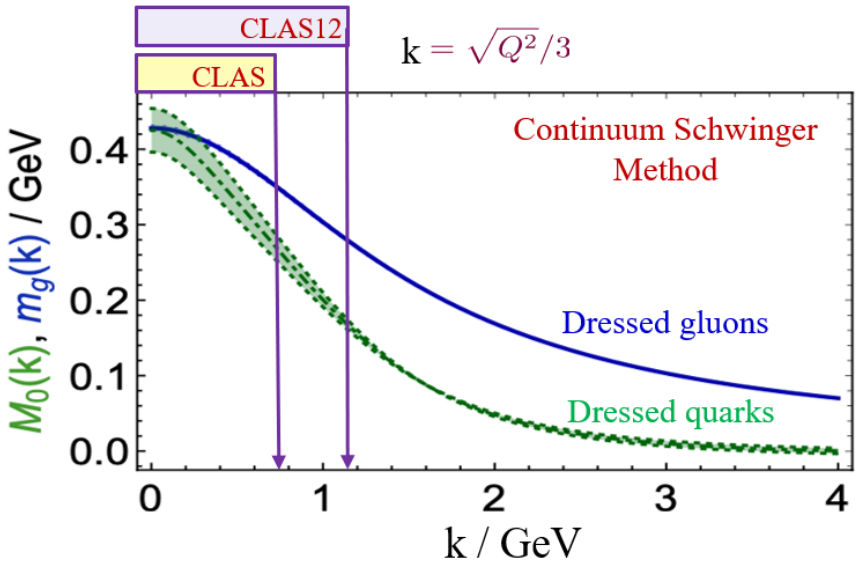
- final cross sections

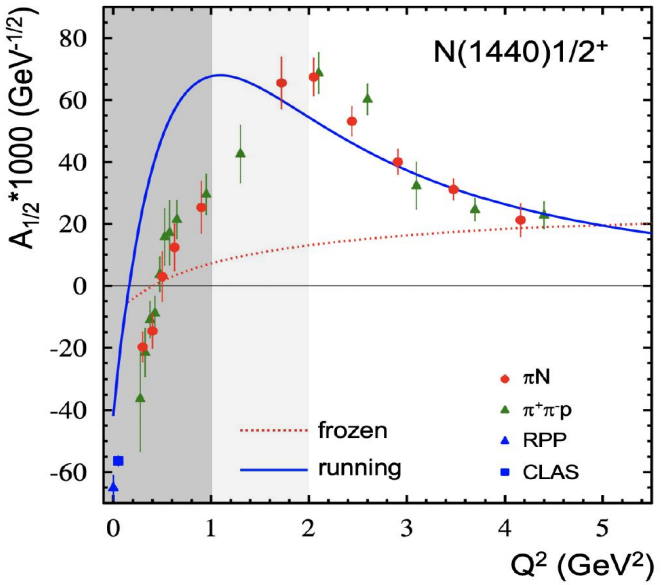
CLAS12

$W \in [1.50, 1.55]$ GeV
$Q^2 \in [6.0, 7.0]$ GeV^2

systematic uncertainties







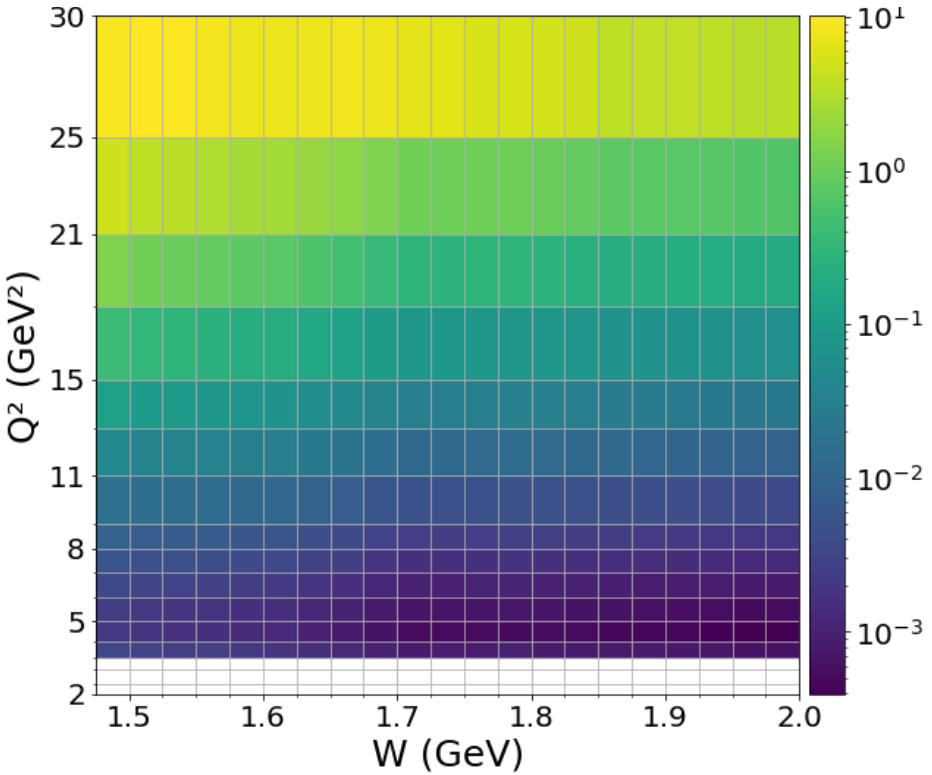
Beam Time Needs for Exclusive $p\pi^+\pi^-$ at CLAS22

Alexis Osmond & Krishna Neupane

Based on RGA Fall 2018 Luminosity of 5.96 10^{34} cm^{-2} s^{-1} at 45 nA and 5 cm LH_2.

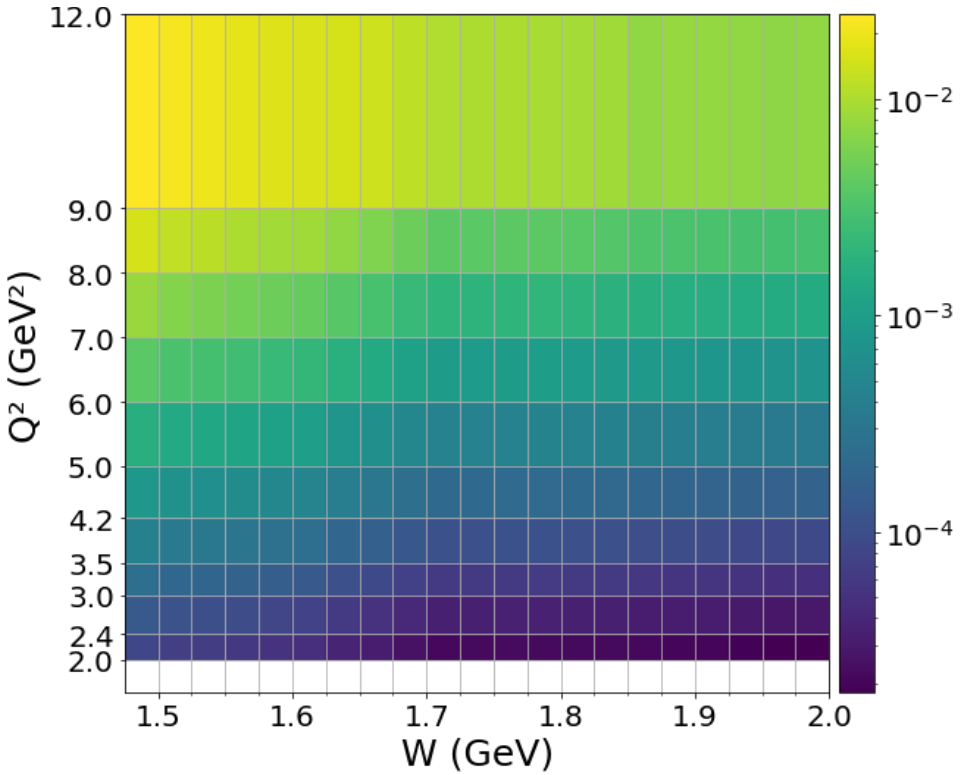
Simulated at 22 GeV Beam Energy

Needed Years at $5.96 \cdot 10^{34}$ (cm^{-2} s^{-1})



Simulated at 10.6 GeV Beam Energy

Needed Years at $5.96 \cdot 10^{34}$ (cm^{-2} s^{-1})



Implementing all analysis cuts (3/2), Golden Run Selection (3), PAC Days (2)

➡ 8 (16) years at $5.96 \cdot 10^{34}$ cm^{-2} s^{-1} or 11 (22) month at $5 \cdot 10^{35}$ cm^{-2} s^{-1} (Stage 1).

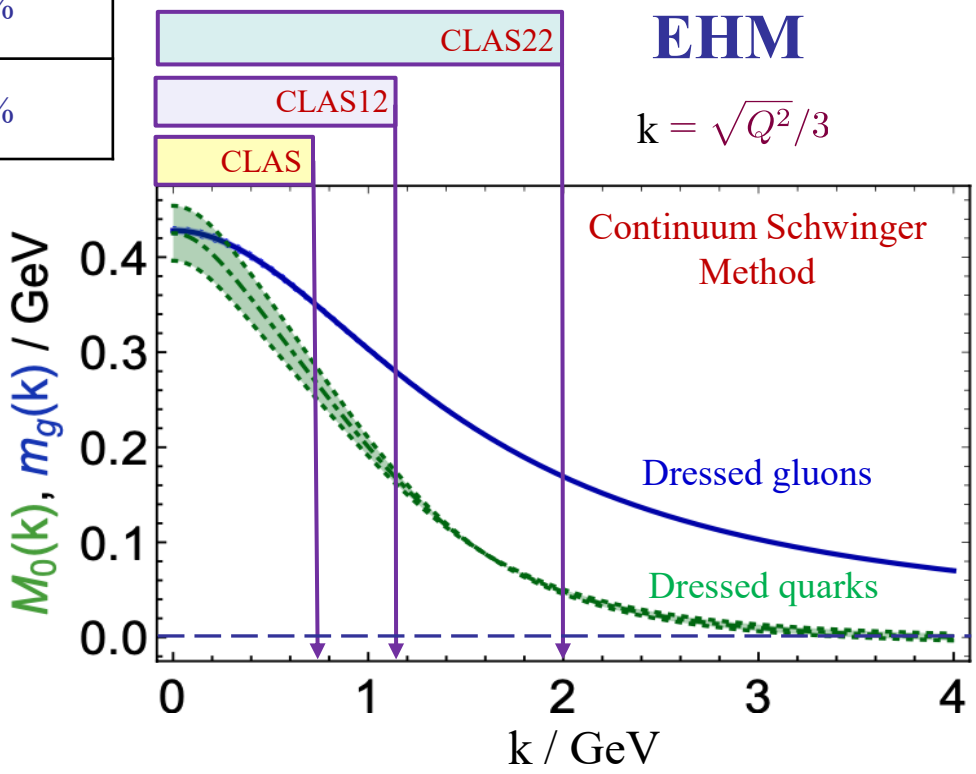
Emergence of Hadron Mass and Structure

	Q^2-coverage of electrocouplings	Range of quark momenta k	Fraction of dressed quark mass at $k<k_{max}$
CLAS	< 5 GeV^2	< 0.8 GeV	30%
CLAS12	< 12 GeV^2	< 1.2 GeV	50%
CLAS22	< 35 GeV^2	< 2.0 GeV	90%

- Beam energy 22 GeV
- Nearly 4π acceptance

Increasing knowledge on running dressed quark mass from the results on γ_vpN* electrocouplings.

Measured γ_vpN* electrocouplings of most prominent N* states of different structure will provide sound evidence for understanding how the dominant part of the hadron mass and the N* structure itself emerge from QCD and will make CEBAF@22 GeV the ultimate QCD-facility at the luminosity frontier.

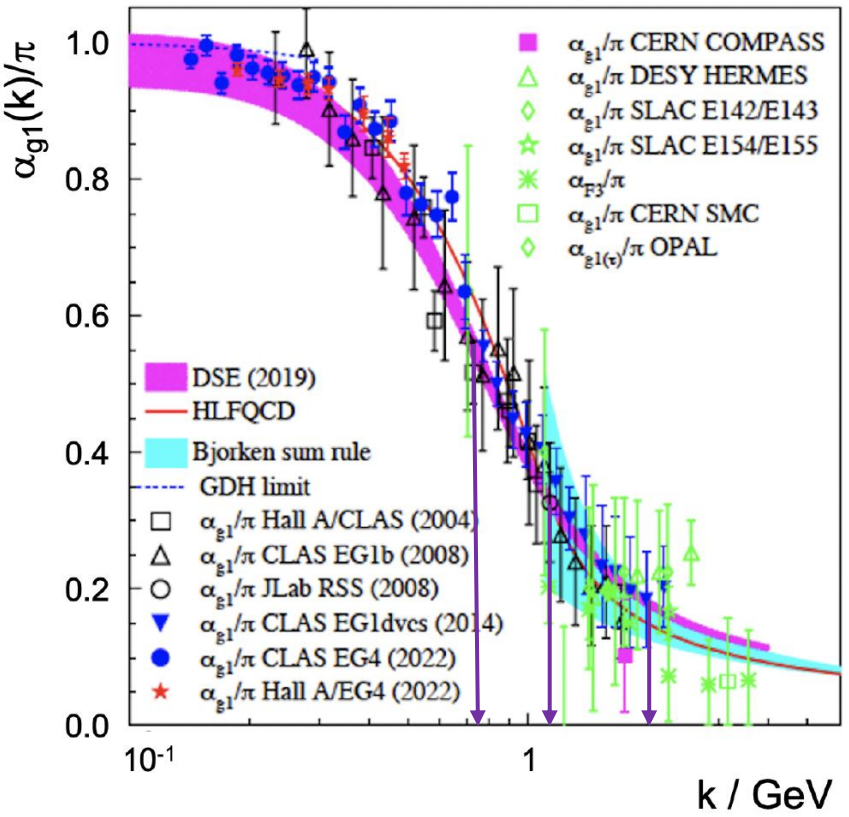


Luminosity "frontier" is the *unique* advantage of JLab.

Emergence of Hadron Mass and Structure

	Q^2-coverage of electrocouplings	Range of quark momenta k	Fraction of dressed quark mass at $k<k_{max}$
CLAS	< 5 GeV^2	< 0.8 GeV	30%
CLAS12	< 12 GeV^2	< 1.2 GeV	50%
CLAS22	< 35 GeV^2	< 2.0 GeV	90%

- Beam energy 22 GeV
- Nearly 4π acceptance



Increasing knowledge on running dressed quark mass from the results on γ_vpN* electrocouplings.

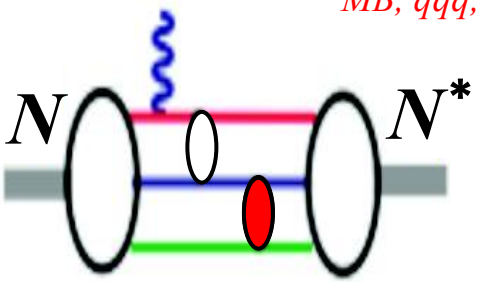
Measured γ_vpN* electrocouplings of most prominent N* states of different structure will provide sound evidence for understanding how the dominant part of the hadron mass and the N* structure itself emerge from QCD and will make CEBAF@22 GeV the ultimate QCD-facility at the luminosity frontier.

Luminosity "frontier" is the *unique* advantage of JLab.

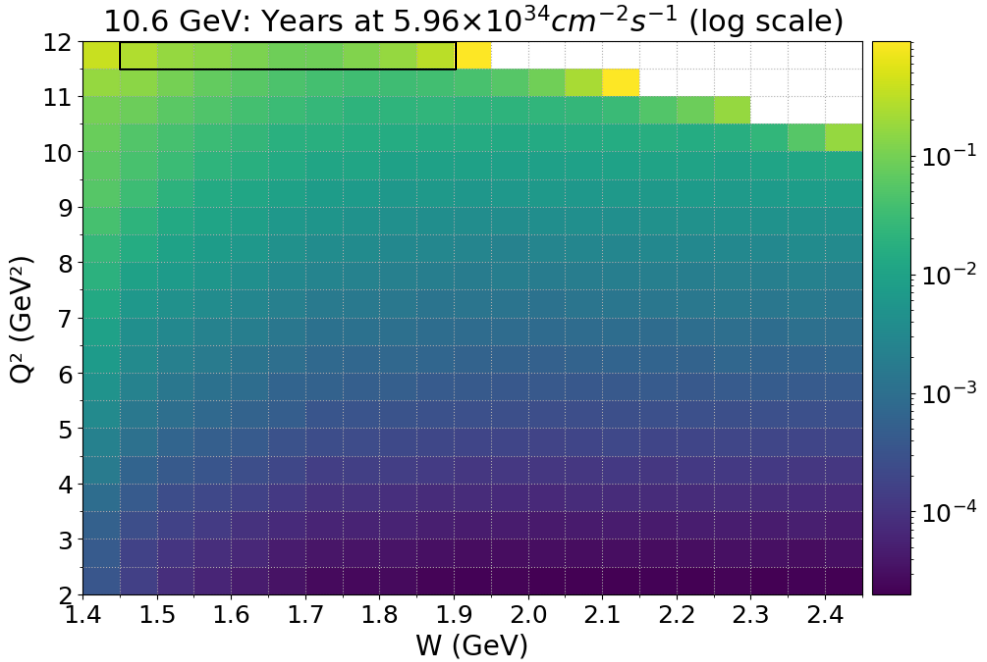
Experimental Measurement of Diquark Correlations

$$F(Q^2) = G_E(Q^2) = \left(1 + Q^2/a^2\hbar^2\right)^{-2}$$

MB, qqq, or qd



$$F(Q^2) = \left(1 + Q^2/a^2\hbar^2\right)^{-1} * \left(1 + Q^2/a_d^2\hbar^2\right)^{-1}$$



High precision cross section measurements.

At high luminosity in 4 months: increased number of Q^2 bins and 2–5 × smaller statistical error bars.